Poincaré–Cosserat Equations for the Lighthill Three-dimensional Large Amplitude Elongated Body Theory: Application to Robotics

Frédéric Boyer, Mathieu Porez, Alban Leroyer

Poincaré-Cosserat equations for Lighthill three-dimensional dynamic model of a self propelled eel devoted to Robotics

Frederic Boyer[1], Mathieu Porez[2] and Alban Leroyer[3]

Technical Report of École des Mines de Nantes and Institut de Recherche en Communication et Cybernétique de Nantes.

Report No. : 07/8/Auto

Abstract

In this article, we propose a dynamic model of the three-dimensional eel swim. This model is analytical and suited to the on-line control of eel-like robots. The proposed solution is based on the Large Amplitude Elongated Body Theory of Lighthill and a working frame recently proposed in [1] for the dynamic modeling of hyper-redundant robots. This working frame was named "macro-continuous" since at this macroscopic scale, the robot (or the animal) is considered as a Cosserat beam internally (and continuously) actuated. This article proposes new results in two directions. Firstly, it achieves an extension of the Lighthill theory to the case of a self propelled body swimming in three dimensions, while including a model of the internal control torque. Secondly, this generalization of the Lighthill model is achieved due to a new set of equations which is also derived in this article. These equations generalize the Poincaré equations of a Cosserat beam to the case of an open system containing a fluid stratified around the slender beam.

Keywords

Swim dynamics, eel-like robots, hyper-redundant locomotion, Lie groups, Lagrangian reduction, Poincaré-Cosserat equations.

1 Introduction

Performances of fishes in terms of manoeuvrability and efficiency are very much higher than those of our technological under-water devices today. As far as underwater manoeuvrability is more particularly concerned, anguilliform fishes like the moray-eel or the eel represent "an optimum" selected by natural evolution. In fact, their high number of internal degrees of freedom (the european eel has more than 120 vertebrae) make of these animals some hyper-redundant locomotors capable of moving with a high agility in very unstructured environments such as the submarine caves of coral reefs. Based on these preliminaries, several "eel like robots" appeared these last years [2, 3, 4]. However, in spite of this increasing interest for these systems, the quest of elongated fish swim models devoted to on-line control (in particular for autonomous navigation) is still a challenging task for bio-mimetic robotics [5]. In fact, computing the interactions between a swimming fish and a fluid is a very involved problem which in itself requires the integration of Navier-Stokes equations coupled with the nonlinear dynamics of a body enduring finite transformations [6, 7, 8, 9]. More simply, several efficient numerical solvers based on the inviscid

[1]**F. Boyer :** EMN, IRCCyN, La Chantrerie 4, rue Alfred Kastler B.P. 20722 - 44307 Nantes Cedex 3 France. Tel. : +00 33 2 51 85 83 08, Fax : +00 33 2 51 85 83 02, E-mail : frederic.boyer@emn.fr.

[2]**M. Porez :** EMN, IRCCyN, La Chantrerie 4, rue Alfred Kastler B.P. 20722 - 44307 Nantes Cedex 3 France. Tel. : +00 33 2 51 85 83 33, Fax : +00 33 2 51 85 83 02, E-Mail : mathieu.porez@emn.fr.

[3]**A. Leroyer** ECN, LMF, 1 rue de la Noë BP 92101 - 44321 Nantes Cedex 3 France. Tel. : +00 33 2 40 37 16 48, E-mail : alban.leroyer@ec-nantes.fr.

fluid model have been proposed during the last decade [10, 11, 12]. Under this restriction, the propulsion of the fish originates only in the exchanges of kinetic amounts of the fluid and its body. Consequently, such models are named "reactive" in [13], and their use is justified by the high Reynolds number that most of the fishes reach when swimming. To these reactive models, a "resistive" model taking into account the effect of the viscosity can be added by invoking the theory of "boundary layer" [10]. However, in spite of these simplifications, these solutions are again too computationally involved to be used for one-line control. Thus, analytical modeling seems to be the most realistic solution for robotics. As far as analytical modeling is concerned, let us remember that in 1960, two models of fish swim appeared which are untill today, considered as references in the field of "bio-fluid-dynamics". The first one, due to Wu [14] is based on the undulating infinite height plate, while the second, due to James Lighthill [13], is based on the Slender-Body Theory (S.B.T.). In both cases, the modeling profits from the particularities of fishes' geometry in order to approximate the 3-D flow around their body by a stratification (horizontal in the first case, vertical in the second) of planar potential ones. Due to its slender geometry, here we essentially consider the fluid dynamics around the eel (and the robot which mimics it) as governed by the S.B.T.. Originally devoted to hydrodynamics of rigid vessels in small perturbations (small angle of attack, small "thickness/length" ratio...) [15], the S.B.T. was extended in [13] to the case of the undulatory swimmers (like the eel) through the "Elongated Body Theory" (E.B.T.), and the "Large Amplitude Elongated Theory" (L.A.E.B.T.) [16], depending if the body endures "small" or "finite amplitudes" deformations respectively. For the purpose of robotics, the L.A.E.B.T. represents an interesting perspective for the on-line control of "eel-like robots". In fact, it gives an analytical simple model of the eel's hydrodynamics while its body achieves realistic swimming gaits of finite amplitude. Nevertheless as far as robotics is concerned, the L.A.E.B.T. is not sufficient in several ways. In fact, like most of his successors until today, his author restricted his study (essentially focused onto the Gray's paradox [17]) to the fluid dynamics submitted to the unsteady boundary conditions due to the imposed motion of the body. Furthermore, the L.A.E.B.T. only deals with the planar straight forward swim. On the other hand, in the article here presented, the case of all the dynamics (fluid + body) is considered. Secondly, the body is self-propelled and not submitted to an imposed motion. Thirdly, the internal dynamics of the control torque law are also solved. Finally, all these problems are solved in real-time (in fact less), and in the case of the three dimensional swim, which until today and to our knowledge, has never been studied.

The solution is based on recent results from [1] and in particular : 1°) on the modeling of the fish body as a non-linear Cosserat beam continuously actuated through a field of internal control torque ; 2°) on a "slice by slice" contact model which combines a resistive model of the drag and viscous forces and a reactive model of inertial (added mass) ones ; 3°) on a fast algorithm which solves the fish head motions and the internal control torques from the given internal strain law applied along the fish body. Furthermore, the solution here presented goes beyond [1] in three ways. Firstly, the reactive model of inertial forces is actually deduced from a balance of the kinetic amounts applied to the fluid and the body considered as a whole. Secondly, coming back to the original Lighthill theory of [16], in order to take into account the influence of the wake onto the fish, this balance is applied to the fluid which is contained in the control volume $\mathcal{D}$ as shown on figure.1. Lastly, in parallel to these modeling works the solution here proposed has been successfully calibrated and tested [18], thanks to comparisons with the Navier-Stokes solver of [9]. Lastly, note that in [19] the anguilliform swim is also modeled as an internally actuated rod, but for the study of the muscle dynamics and in the case of the planar anguilliform swim.

These results are derived from the extension of a variational calculus historically initiated by Poincaré [20] and today known as the foundation of the Lagrangian reduction theory [21, 22, 23].

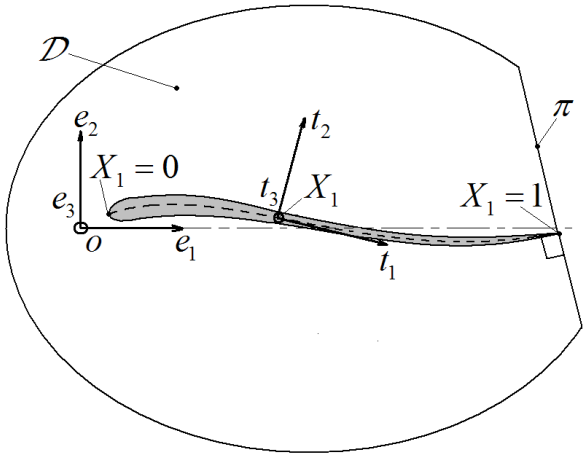

FIG. 1 – The volume control $\mathcal{D}$ used by Lighthill to isolate the rotational wake from the potential flow laterally bounding the body. Note that π is the plane perpendicular to the backbone passing through the trailing edge of the caudal fin.

This calculus is one of the essential Geometric Mechanics tools thanks to which many of the recent advances have been produced in the field of bio-mimetic locomotion (see [24, 25, 26]). In the case of the eel swim, we will first recall this calculus to the case of a Cosserat beam [27]. Then, due to the slender-body assumption, the flow will be stratified in $\mathcal{D}$, and the Hamilton principle extended to the case of this stratified fluid flowing out of $\mathcal{D}$. We will derive two dynamics from this principle. The first ones named "internal-dynamics" are merely the partial differential equations (p.d.e.'s) which govern the internal control torques. The second dynamics, named "external dynamics", rule the eel's head motions driven by the internal shape law. Finally, these results were obtained in the working-frame of a research project whose purpose is to design and control an eel-like robot capable of swimming in the three dimensions. This robot is an assemblage of pairs of parallel platforms or "vertebrae". Two consecutive vertebrae are connected by parallel kinematics which are equivalent to a universal two degrees of freedom (d.o.f.) joint, one d.o.f. corresponding to the pitch angle and the second, to the yaw.
Lastly, the article is structured as follows. In section 2, we briefly recall the Lighthill theory of anguilliform swim. Section 3 is devoted to the Cosserat beam theory from the point of view of Poincaré variational calculus on Lie groups. In section 4, starting from the E.B.T., the flow laterally surrounding the slender body is stratified into a field of fluid slices transverse to the beam. Based on this stratification, the Poincaré-Cosserat construction is extended to the case of a swimming slender fish in section 5, which ends with the p.d.e.'s of the fish dynamics. These equations encode all the information about the fluid-structure interactions and the internal forces of the beam body. Then, in section 6, the previous p.d.e.'s are reconsidered in order to deduce the external head's dynamics, i.e. the dynamics of the fish head when its body is submitted to an imposed internal strain law. Then the resulting model is used in section 7 for the purpose of simulation. The same section gives a three-dimensional numerical example validated in [18] with a Navier-Stokes solver. Finally, the article ends with concluding remarks (section 8).

2 Elongated body theory of Lighthill

Firstly we recall the great lines of the Lighthill's modelling (E.B.T. and L.A.E.B.T.) where E.B.T. can be seen as a linear perturbation theory of the original S.B.T. with respect to the body deformations of the fish. Before all, the body is considered as slender with a rounded nose and

a tail (caudal fin) modeled by a sharp trailing edge. Secondly, the fluid is assumed to be perfect (inviscid) and irrotational everywhere except in the wake which is modeled by a free vortex sheet. Thirdly, in order to circumvent the complex modeling of the wake, Lighthill restricts his considerations to the fluid contained in an hemispheric control volume $\mathcal{D}$ including the eel's body and separated from the wake by the plane π passing through the caudal fin and perpendicular to the eel's backbone (cf. figure 1). In these conditions, only the kinetic exchanges of the fluid contained in $\mathcal{D}$, where the flow is assumed to be potential, with the wake are considered. Finally, because the fluid has no viscosity, the forces applied on the body have a pure inertial nature and can be modeled by some "added" or "virtual inertia" in accordance to what Lighthill named a "reactive" model, and that he opposed to a "resistive" one as required by the study of low Reynolds swimmers like worms [28]. With these choices, Lighthill first considered in [13] a slender fish maintaining its head fixed in a steady flow of velocity U by imposing to its body a given undulation law of small amplitude. Then, he extended his study in reference [29] to the case of a slender body enduring planar finite amplitude undulations in a fluid at rest far from the fish. In this Large Amplitude Elongated Body Theory, like in the small perturbations one (or Elongated Body Theory), each slice of the fluid stays at rest axially but is laterally accelerated by the beam cross sections as it sweeps past the body. Hence, the fluid kinetic amounts of the slice grow along the beam (from the head to the tail) before to be shed into the wake, so generating the fish thrust by reaction. Beyond this amplification mechanism, Lighthill gave in his L.A.E.B.T. of [29] the following expression for the forces applied to a slender inextensible undulating body of normalized length, swimming along e_1 (cf. Figure 2.) :

$$Te_1 + Le_2 = -\frac{\partial}{\partial t}\int_0^1 mV_2 t_2 dX_1 + \left[mV_2V_1t_2 - \frac{1}{2}mV_2^2t_1\right]_{X_1=1}, \tag{1}$$

where, (o, e_1, e_2, e_3) is a fixed Galilean frame, while $(t_1, t_2, t_3)(X_1)$ is the ortho-normed mobile basis attached to the body cross section c_{X_1} of added mass $m(X_1)$, positioned at the distance X_1 along the backbone w.r.t. the nose, with t_1 being tangent to the backbone, and t_3 normal to the swimming plane. Finally, "$(V_1t_1 + V_2t_2)(X_1)$" denotes the velocity of c_{X_1}. Physically, we find in (1) and from left to right : 1°) the thrust (T) and lateral (L) forces (the eel swimming in straight line), 2°) the rate of change of fluid momentum within $\mathcal{D}$ due to the body motion, 3°) the rate of change of momentum within $\mathcal{D}$ due to momentum transport across the plane π. Moreover, following Lighthill's conclusions, this is this last contribution whose time-averaged value is non null, which is essentially at the origin of the undulating fish thrust.

Before closing this presentation of the Lighthill model, let us remark that (1) is based on the fact that the axial (i.e. along the fish backbone) perturbations of the velocity field of the fluid w.r.t. the fish is negligible due to the slenderness of its body. Nevertheless, if this can be legitimated rigorously from perturbation theory in the case of the E.B.T. [13], this is not the case when the amplitude of the fish undulations increase. In fact, the curvature of the fish backbone will generate some mixing of the transverse fluid slices incompatible with the S.B.T. Hence, the extension of the E.B.T. to the Large Amplitude E.B.T. introduces a sort of heuristic, summarized as follows by the author. The fluid kinematics from which the added mass density is computed - which generates the density of hydrodynamic force applied onto the finite deformed fish configuration - are defined slice by slice as if each of the fish sections c_{X_1} would be axially prolonged by an infinite cylinder of constant section moving with the transverse motion of c_{X_1}. Lastly, let us point out that Lighthill derived (1) through the kinetic energy conservation law applied to the fluid in $\mathcal{D}$. Furthermore, in this balance, all the terms of (1) appear as some inertial forces. Hence, the L.A.E.B.T. should be founded on a variational calculus where all the hydrodynamic forces of (1) can be derived from the fluid kinetic energy. This is one of the purposes of this article to contribute to these foundations.

3 Poincaré equations of an internally actuated Cosserat beam

In all the article, we use the following notations. The contracted product of two tensors is denoted by a point, $\otimes$ is the usual tensor product and $\times$ the cross product in $\mathbb{R}^3$. For any $W \in \mathbb{R}^3$, $\widehat{W} = W^\wedge$ is the skew-symmetric tensor such that $\widehat{W}.X = W \times X, \forall X \in \mathbb{R}^3$ and $\widehat{W}^\vee = (W^\wedge)^\vee = W$. Any tensor field can depend on time in two ways as its time evolution is known (i.e. imposed or computed by integration) or only ruled by the dynamics. In the first case the time is explicitly indicated as an argument, while it does not appear in the second case. Finally, if $\mathcal{V}$ denotes a closed set of $\mathbb{R}^n$, then ∂V is its boundary set, while $d\mathcal{V}$ and $d\partial\mathcal{V}$ are respectively the volume and surface elements of $\mathcal{V}$. Finally following the notations of the geometrically exact beam theory of [30], the spatial tensors are denoted by small characters while the material ones are denoted by large ones. Lastly, the notations of the previous section will be systematically used (and augmented) in all the following.

3.1 Basic picture

We first recall the usual Poincaré-Cosserat picture as it is proposed in [27]. For the moment, we ignore the fluid and just consider that the fish is submitted to any arbitrary external load. Due to its slenderness, the fish can be modeled as a beam of unit length where the cross sections $c_{X_1}, X_1 \in [0,1]$ remain rigid while moving, i.e. by a one dimensional Cosserat medium whose configuration space is defined by the functional set of curves in the Lie group $SE(3)$:

$$\mathcal{C} \triangleq \{g : X_1 \in [0,1] \mapsto g(X_1) \in SE(3)\}. \tag{2}$$

In a tensorial representation, any $g(X_1)$ is defined by the homogeneous transformation :

$$g(X_1) = \begin{pmatrix} R(X_1) & r(X_1) \\ 0 & 1 \end{pmatrix}, \tag{3}$$

where $R(X_1)$ and $r(X_1)$ are respectively the rotation and position operators which map the material frame (O, E_1, E_2, E_3) onto the current mobile frame $(G, t_1, t_2, t_3)(X_1)$ attached to the X_1 cross section of mass center $G(X_1)$ (cf. figure 3).

Now, the Poincaré-Cosserat construction consists in deriving from a Lagrangian approach the dynamics of the beam directly on the definition (2) of the beam configuration space. Technically, this is achieved by applying the extended Hamilton principle [31] :

$$\delta \int_{t_1}^{t_2} L_b dt = \delta \int_{t_1}^{t_2} \int_0^1 \mathcal{L}_b dX_1 dt = \int_{t_1}^{t_2} \delta W_{ext} dt, \tag{4}$$

where δ denotes any variation applied along the trajectory of the system while the configuration at the two ends of $[t_1, t_2]$ are maintained fixed, and δW_{ext} is the virtual work produced by the (non-conservative) external loads. Furthermore, L_b and $\mathcal{L}_b$ respectively denote the Lagrangian and the Lagrangian density of the beam free of external load. In the Poincaré-Cosserat approach, $\mathcal{L}_b$ is directly defined as a function of the cross sections transformations and their space and time derivatives $\mathcal{L}_b\left(g, \frac{\partial g}{\partial X_1}, \frac{\partial g}{\partial t}\right)$; and not, like in the case due to Lagrange, as a function of any parametrization of the g's in $\mathbb{R}^6$. Then, let us remember that the variation is applied onto any motion in $\mathcal{C}$ while the space and time variables are maintained fixed. In fact, $\delta t = 0$ in accordance to the D'Alembert principle of virtual works, while $\delta X_1 = 0$ since the variable X_1 is a material (configuration independent) label (note here that this imposes to $\delta.$ to follow c_{X_1} along any virtual displacement, a property that will play a crucial role in the generalization of this construction to the fluid, see B.4 in the appendix).

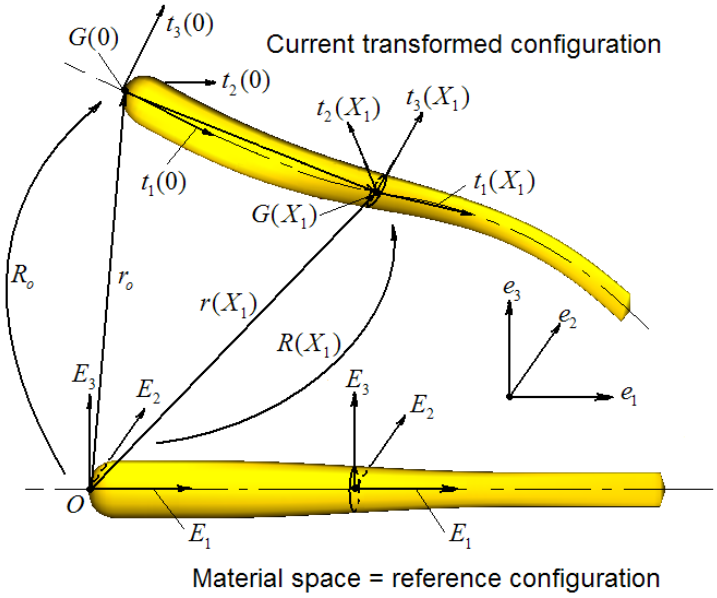

FIG. 2 – Basic picture of a Cosserat beam.

3.2 Reduced dynamics of a one-dimensional Cosserat medium

Now, let us define the following space and time twist fields :

$$\eta \triangleq g^{-1}\frac{\partial g}{\partial t}(X_1) \ , \xi \triangleq g^{-1}\frac{\partial g}{\partial X_1}(X_1), \tag{5}$$

where η and ξ are both defined in the $(E_1, E_2, E_3, \widehat{E}_1, \widehat{E}_2, \widehat{E}_3)$ basis of $se(3)$, in agreement with the "material setting" of the rigid body geometry [32]. Furthermore, in the following we identify $se(3)$ with $\mathbb{R}^6$, and η and ξ with :

$$\eta = \begin{pmatrix} (R^T.(\partial R/\partial t))^\vee \\ R^T.(\partial r/\partial t) \end{pmatrix} \triangleq \begin{pmatrix} \Omega \\ V \end{pmatrix} \ , \xi = \begin{pmatrix} (R^T.(\partial R/\partial X_1))^\vee \\ R^T.(\partial r/\partial X_1) \end{pmatrix} \triangleq \begin{pmatrix} K \\ \Gamma \end{pmatrix}, \tag{6}$$

where Ω, V (respectively K and Γ) respectively denote the material angular and linear velocity (respectively the material "curvature-twist" and tangent vector) fields along the beam. Then, introducing the definitions (5) into the Lagrangian density of the beam, allows one to rewrite (4) as :

$$L_b = \int_0^1 \mathcal{L}_b \left(g, \frac{\partial g}{\partial X_1}, \frac{\partial g}{\partial t} \right) dX_1 = \int_0^1 \mathfrak{L}_b(g, \eta, \xi) dX_1, \tag{7}$$

where $\mathfrak{L}_b$ is a new function named "reduced Lagrangian density" (in the Lie algebra of $SE(3)$), when it does not depend explicitly of the transformation g. In fact, this property is named "left invariancy" and traduces the symmetry of the dynamics as seen by an observer attached to the beam material. In the rest of this section, we shall assume that the Lagrangian of the beam free of load is left invariant and we will see later how this is actually the case when we consider the eel swimming in a perfect fluid. Now, let us derive the beam dynamics by applying the variational principle (4) with L_b defined by (7). For this, we have to invoke the constraints of variation at fixed time and material label :

$$\delta\frac{\partial g}{\partial t} = \frac{\partial \delta g}{\partial t} \ , \delta\frac{\partial g}{\partial X_1} = \frac{\partial \delta g}{\partial X_1}, \tag{8}$$

where $\delta\zeta = g^{-1}\delta g \in se(3)$ is a field of material variation of g, with $\delta\zeta(t_1) = \delta\zeta(t_2) = 0$. Then inserting "$\delta g = g\delta\zeta$" into (8.a) and (8.b) gives the following relations, as historically revealed by Poincaré [20], relations which play a key role in the variational calculus on Lie groups :

$$\delta\eta = \frac{\partial\delta\zeta}{\partial t} + ad_{*\eta}(\delta\zeta) \ , \ \delta\xi = \frac{\partial\delta\zeta}{\partial X_1} + ad_{*\xi}(\delta\zeta). \tag{9}$$

Finally, applying the standard uses of variational calculus to (4), with (9) running before the usual by part integrations (here in "space" and "time"), gives the Poincaré equations of a Cosserat-beam in the material setting (see Appendix A) :

$$\frac{\partial}{\partial t}\left(\frac{\partial\mathfrak{L}_b}{\partial\eta}\right) - ad^*_\eta\left(\frac{\partial\mathfrak{L}_b}{\partial\eta}\right) + \frac{\partial}{\partial X_1}\left(\frac{\partial\mathfrak{L}_b}{\partial\xi}\right) - ad^*_\xi\left(\frac{\partial\mathfrak{L}_b}{\partial\xi}\right) = \overline{F}, \tag{10}$$

with the boundary conditions (also deduced from (4)) :

$$\frac{\partial\mathfrak{L}_b}{\partial\xi}(0) = F_- \ , \text{ and : } \frac{\partial\mathfrak{L}_b}{\partial\xi}(1) = -F_+, \tag{11}$$

where, we assume that the external load is defined by the density field of wrench $X_1 \in]0,1[\mapsto \overline{F} \in se(3)^*$, and the two boundary wrenches $F_- \in se(3)^*$ and $F_+ \in se(3)^*$ respectively applied onto the first and last cross section of the beam, i.e., we assume that $\delta W_{ext} = \int_0^1 \overline{F}.\delta\zeta dX_1 + F_-.\delta\zeta(0) + F_+.\delta\zeta(1)$ in (4). Finally, these external wrenches generally depend on the beam configuration. Nevertheless, when this is not the case, the external load is said to be left invariant. This is particularly the case of the most of the contact forces involved in animal locomotion. In the following, we will see that because of their inertial nature, all the contact forces of the reactive model (1) can in fact be directly derived from the left hand side (l.h.s.) of (4). However, we shall use in the simulations of 7 the external load of the right hand side (r.h.s.) of section (4) in order to improve the L.A.E.B.T. of some corrections.

3.3 Application to an internally actuated Cosserat beam

Following [1], we propose to model the hyper-redundant eel-robot as a Cosserat beam submitted to a field of curvature $K_d(t) : X_1 \in [0,1] \mapsto K_d(X_1,t) \in so(3)$, imposed at each instant t along its back-bone. Furthermore, the rigid cross sections of the beam, model the parallel platforms (which mimic the vertebrae of the animal) linked together through the pitch-yaw universal joints (see introduction). With these choices, the internal beam kinematics has to satisfy the following constraints :

$$\forall X_1 \in]0,1[: \ K(X_1) = K_d(X_1,t) \ , \ \Gamma(X_1) = E_1, \tag{12}$$

where the rotational part of (12) (with $K_d(t) = K_{d,2}(t)E_2 + K_{d,3}(t)E_3$) stands for the desired control inputs, while the translational one stands for the "inextensibility" and "Kirchhoff constraints" of beam theory [33]. Finally, note that (12) can be rewritten as the single space-twist relation :

$$\xi(X_1) - \xi_d(X_1,t) = 0, \forall X_1 \in]0,1[, \tag{13}$$

with $\xi_d = (K_d^T, E_1^T)^T$. Once the internal constraints so defined, we are now able to fix the Lagrangian density of (7) as :

$$\mathfrak{L}_b(\eta,\xi,t) = \mathfrak{T}_b(\eta) - \mathfrak{U}_b(\xi,t), \tag{14}$$

where we introduced :

– The left invariant density of internal energy $\mathfrak{U}$ imposed by the constraints as :

$$\mathfrak{U}_b(\xi,t) = \lambda.(\xi - \xi_d(t)), \tag{15}$$

where $\lambda : X_1 \in [0,1] \mapsto \lambda(X_1) \in se(3)^*$ is the field of internal wrench which forces the constraint (13), i.e. $\lambda = (C^T, N^T)^T$ where C and N are the density fields of internal torque ($C_\alpha = C.E_\alpha, \alpha = 2,3$ are the two control torque laws) and internal reaction force respectively.

– The left invariant density of beam kinetic energy $\mathfrak{T}_b$, defined by :

$$\mathfrak{T}_b(\eta) = \frac{1}{2}\eta.(\mathbb{J}_b.\eta), \tag{16}$$

and $\mathbb{J}_b(X_1)$ is the 6×6 density of material inertia tensor, which in the case of an elliptic cross-sectional profile is given by :

$$\mathbb{J}_b = \begin{pmatrix} J_b & 0 \\ 0 & M_b \end{pmatrix}, \tag{17}$$

with : $J_b = \rho_b(J_1E_1\otimes E_1 + J_2E_2\otimes E_2 + J_3E_3\otimes E_3)$, $M_b = \rho_b A(E_1\otimes E_1 + E_2\otimes E_2 + E_3\otimes E_3)$, ρ_b is the mass per unit of beam volume, and A, $J_i, (i=1,2,3)$ are the area and geometric moments about $t_i, (i=1,2,3)$ of the X_1 beam cross section respectively.

Finally, let us insert (14) with (16) and (15), into (10)-(11) gives :

$$\frac{\partial(\mathbb{J}_b.\eta)}{\partial t} - ad^*_\eta(\mathbb{J}_b.\eta) - \frac{\partial\lambda}{\partial X_1} + ad^*_\xi(\lambda) = \overline{F}, \tag{18}$$

with the boundary conditions :

$$\lambda(0) = F_- \text{ , and : } \lambda(1) = -F_+. \tag{19}$$

Then, identifying $se(3)$ and $se(3)^*$ to $\mathbb{R}^6$, the explicit expression of the co-adjoint action of any twist $\Xi = (\Omega^T, V^T)^T \in se(3)$ onto any wrench $\Theta = (C^T, N^T)^T \in se(3)^*$ is given by [34] :

$$ad^*_\Xi(\Theta) = \begin{pmatrix} C\times\Omega + N\times V \\ N\times\Omega \end{pmatrix}, \tag{20}$$

Furthermore, if we denote by $\mathbb{J}_b.\eta = \partial\mathfrak{T}_b/\partial\eta = (\Sigma_b^T, P_b^T)^T$ the density of material kinetic wrench along the body and by $\overline{F} = (\overline{C}^T, \overline{N}^T)^T$, the density of external material wrench, we find after simple computations starting from (18) and using (20) :

$$\frac{\partial}{\partial t}\begin{pmatrix}\Sigma_b \\ P_b\end{pmatrix} + \begin{pmatrix}\Omega\times\Sigma_b + V\times P_b \\ \Omega\times P_b\end{pmatrix} = \frac{\partial}{\partial X_1}\begin{pmatrix}C \\ N\end{pmatrix} + \begin{pmatrix}K\times C + \Gamma\times N \\ K\times N\end{pmatrix} + \begin{pmatrix}\overline{C} \\ \overline{N}\end{pmatrix}. \tag{21}$$

Finally, the field equations (21), once completed with the boundary conditions (19) which can now be detailed, with $F_\pm \triangleq (C_\pm^T, N_\pm^T)^T$, as :

$$\begin{pmatrix}C(0) \\ N(0)\end{pmatrix} = \begin{pmatrix}C_- \\ N_-\end{pmatrix}, \begin{pmatrix}C(1) \\ N(1)\end{pmatrix} = -\begin{pmatrix}C_+ \\ N_+\end{pmatrix}, \tag{22}$$

plus the internal constraints (12), and the definitions (6), form a closed form of the internally actuated Cosserat beam dynamics.

3.4 Computational algorithm

From the beam theory point of view, the closed form (6,12,21,22) corresponds to the dynamics of a torque-actuated Kirchhoff inextensible beam [33] once they are stated in the larger configuration space (2) of Reissner-Timoshenko beams [35]. In the passive case, such a closed form can be solved by applying the geometrically-exact finite-element method of Simo [36, 33]. Here, we will not follow this approach but rather a computational algorithm recently proposed in [1] for the dynamics of hyper-redundant robots ("trunk robots", "snake-like" or "eel-like" robots...). This algorithm is based on a slight different formulation from (6,12,21,22) that we now detail as following. Firstly, let us explicitly force the constraints (12) in (21) which can then be rewritten in the spatial setting (we use small characters for denoting the spatial counterparts of the material tensors previously defined), as :

$$\frac{\partial}{\partial t}\begin{pmatrix} \sigma_b \\ p_b \end{pmatrix} = \frac{\partial}{\partial X_1}\begin{pmatrix} c \\ n \end{pmatrix} + \begin{pmatrix} t_1 \times n \\ 0 \end{pmatrix} + \begin{pmatrix} \overline{c} \\ \overline{n} \end{pmatrix}. \tag{23}$$

Secondly, as far as the boundary conditions are concerned, they are unchanged, and we can write them in the spatial setting as :

$$\begin{pmatrix} c(0) \\ n(0) \end{pmatrix} = \begin{pmatrix} c_- \\ n_- \end{pmatrix}, \begin{pmatrix} c(1) \\ n(1) \end{pmatrix} = -\begin{pmatrix} c_+ \\ n_+ \end{pmatrix}. \tag{24}$$

Thirdly, (6) is used to rewrite the constraints (12) as :

$$\frac{\partial R}{\partial X_1} = R.\widehat{K}_d(t) \quad , \quad \frac{\partial r}{\partial X_1} = R.E_1 = t_1. \tag{25}$$

Hence, this second formulation is obtained in two steps : 1°) the Hamilton principle (4) is developed on the Reissner-Timoshenko configuration space, i.e. with any $\delta\xi$ defined by (9.b), 2°) once all the variational calculus is achieved, the constraint $\xi = \xi_d$ is forced. Now, the reader familiar with "robot dynamics" will recognize in ((23)-(25)) the (closed) Newton-Euler formulation of manipulators [37], here extended to the case of a continuous locomotive robot where the body index is replaced by the cross section label X_1. In this context, we proposed in [1] a fast algorithm enable to solve the following dynamic problem : "Compute the head motion of the beam (i.e. that of $(G, t_1, t_2, t_3)(0)$), and the internal torque law C, from the knowledge of the internal strain law $K_d(t)$". From the point of view of robotics, this algorithm is nothing but a continuous version of the Newton-Euler computed torque algorithm of manipulators [38], here extended to the case of locomotion. In order to illustrate this, let us consider the more simple case of a continuous manipulator rigidly linked in $X_1 = 0$ to a mobile platform of given motion $t \mapsto g_o(t)$ and submitted to the known wrench $(c_+^T, n_+^T)^T$ at the other tip. In this case, the first natural boundary condition (24.a) is replaced by the geometric one : $g(X_1 = 0) = g_o(t)$ and at each current time t, the algorithm first computes the current configuration of the beam by space forward integrating (25) (i.e. w.r.t. X_1 and from the earth to the tip), which plays the role of a continuous kinematic model for the manipulator. Then, time differentiating (25) twice, gives the continuous models of the Galilean beam velocities and accelerations [1], that the algorithm forward space integrates too, in order to compute the desired velocity and acceleration fields along the beam. Once all these kinematics known, the p.d.e.'s (23) are backward space integrated at t fixed (with (24.b) as boundary conditions), in order to obtain the internal force n and finally the control torque law C which insures $(K_d, \partial K_d/\partial t, \partial^2 K_d/\partial t^2)(t)$ with $g(0) = g_o(t)$, $(\partial g/\partial t)(0) = \dot{g}_o(t) \triangleq (\mu_o g_o)(t)$, and $(\partial^2 g/\partial t^2)(0) = \ddot{g}_o(t) \triangleq ((\dot{\mu}_o + \mu_o^2) g_o)(t)$ (we denote by a dot the time derivative of a function which only depends on time). Hence, in the case of a continuous manipulator, the algorithm of [1] can be summarized as follows :

$$C(t) = G_{int}\left((g_o, \mu_o, \dot{\mu}_o)(t), \left(K_d, \frac{\partial K_d}{\partial t}, \frac{\partial^2 K_d}{\partial t^2}\right)(t)\right), \tag{26}$$

where G_{int} formally denotes the map which numerically computes the internal torques. In the case of a continuous locomotor (like a swimming eel-like robot), the previous algorithm can be extended by replacing the imposed time evolution $t \mapsto g_o(t)$ (i.e. this of the external d.o.f.), by a dynamic model or "external dynamics", which encodes the effect on the head-frame $(G, t_1, t_2, t_3)(X_1 = 0)$ of all the contact forces applied by the environment onto the animal while it moves its internal d.o.f.. In our case, these external dynamics can be formally written as follows :

$$\begin{pmatrix} \dot{\mu}_o \\ \dot{g}_o \end{pmatrix} = \begin{pmatrix} G_{ext}\left(g_o, \mu_o, \left(K_d, \frac{\partial K_d}{\partial t}, \frac{\partial^2 K_d}{\partial t^2}\right)(t)\right) \\ \mu_o g_o \end{pmatrix}. \tag{27}$$

In the following, we propose an efficient way of computing G_{ext} for a swimming elongated fish. As it is proposed in [1], this computation ends with the formula $G_{ext} = \mathbb{I}_o^{-1}.\mathbb{F}_o$, where $\mathbb{I}_o$ is the 6×6 tensor (with respect to the nose $c_{X_1=0}$) of the inertia and added masses of all the mater (body+fluid) contained at each instant in $\mathcal{D}$, while $\mathbb{F}_o$ is the wrench of all the inertial and external forces applied onto the robot. As for G_{int}, it is worth noting here, that in accordance with the Newton-Euler formalism of robot dynamics [38, 39, 40], G_{ext} (i.e. $\mathbb{I}_o$ and $\mathbb{F}_o$), will be computed under an implicit form, giving its programming simplicity and computational efficiency to the approach. Finally, this algorithm is based on an extension of the Poincaré-Cosserat equations to the fluid laterally surrounding the beam, that we are now going to detail.

4 Basic picture of the anguilliform swim

The extension of the previous mathematical construction to the fluid around the beam is based on the Lighthill model of anguilliform swim. As this model is first based on the Elongated Body Theory (E.B.T.), we start from this context (subject of the two following subsections) but here extended to the three dimensional case, and we will reconsider (in subsection 4.3) the case of a 3D Large Amplitude E.B.T. or L.A.E.B.T. (as first evoked at the end of section 2).

4.1 Fluid kinematics

Let us first recall that in the E.B.T. the beam is assumed to endure small deformations. Then, if we prolong its material axis in the front of its nose by a rigid line supported by $-t_1(0)$, X_1 now belongs to $]-\infty, 1]$, and for any point $x \in \mathcal{D}$ near to the body, a label $X_1 \in]-\infty, 1]$ exists such that $x = r(X_1) + (X_2 t_2(X_1) + X_3 t_3(X_1)) \triangleq r(X_1) + \overline{x}_{X_1}$. Then, following [13], due to the slenderness (and small perturbations of the body shape) of the swimming fish, the three dimensional potential flow in $\mathcal{D}$ can be approximated by a one-dimensional stratification of planar potential flows. By "stratification" we here understand a continuous juxtaposition of fluid slices, each one of them being defined as the part of fluid contained at each instant in the geometric section $s_{X_1}(t)$ which prolongs the current beam cross section configuration $c_{X_1}(t)$ (see Figure 3). More precisely, at the first order of approximation w.r.t. the small quantities of the problem, the hydrodynamic forces exerted onto a slender undulating fish are derived from the unsteady Bernoulli pressure law with the following approximation of the three-dimensional velocity potential ϕ :

$$\forall x \in \mathcal{D}, \phi(x) = \phi(r(X_1) + \overline{x}_{X_1}) \simeq \overline{\phi}_{X_1}(\overline{x}_{X_1}), \tag{28}$$

where $\overline{\phi}_{X_1} = 0$ if $X_1 \in]-\infty, 0]$, while if $X_1 \in]0, 1]$, each $\overline{\phi}_{X_1}$ is solution of the planar Neumann problem :

$$\Delta\overline{\phi}_{X_1} = 0, \text{ on } s_{X_1}(t) - c_{X_1}(t), \tag{29}$$

where the fluid is at rest far from the body and submitted to the following boundary conditions on $\partial c_{X_1}(t)$:

$$\frac{\partial\overline{\phi}_{X_1}}{\partial\overline{n}_{X_1}} = ((V_2t_2 + V_3t_3)(X_1) + (\Omega_1t_1)(X_1) \times \overline{x}_{X_1}) .\overline{n}_{X_1}, \tag{30}$$

with $\overline{n}_{X_1}$, the outward normal to the planar beam cross section profile $\partial c_{X_1}(t)$ which verifies : $n(x = r(X_1)+\overline{x}_{X_1}) \simeq \overline{n}_{X_1}(\overline{x})$ all along the beam except on the rounded nose, where the slender-body assumption introduces a local negligible error [41]. Finally, in the E.B.T. the fluid kinematics are replaced by those of a one dimensional stratified medium of fluid slices staying axially (i.e. along the eel backbone) at rest with respect to the ambient space but sweeping past the stratified space of beam slices.

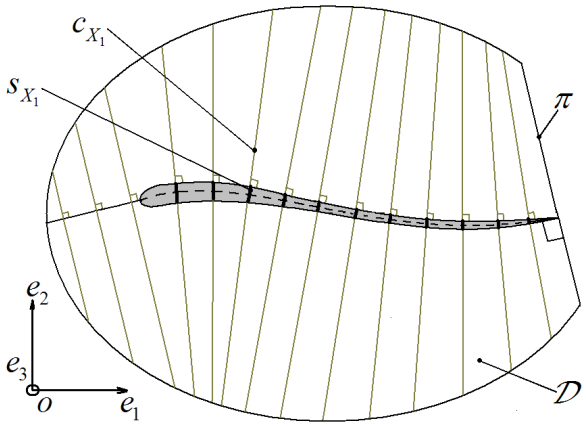

FIG. 3 – Stratification of the fluid flow in $\mathcal{D}$.

4.2 Fluid kinetics

In order to extend the Poincaré picture from the Cosserat beams to the E.B.T. of fluid mechanics, the previous reduction (stratification of kinematics) should be pushed forward to the kinetics. For that purpose, we use the Kirchhoff principle for potential flow around a rigid body [42], where in our case the basic rigid elements are the beam cross sections pushing laterally the fluid in the slices according to (28-30). In this context, the set of planar potentials defined by (28-30) can be rewritten in the Kirchhoff form as :

$$\forall X_1 \in [0, 1] \ , \overline{\phi}_{X_1}(\overline{x}_{X_1}) = \Psi_{1,X_1}\Omega_1 + \Psi_{2,X_1}V_2 + \Psi_{3,X_1}V_3, \tag{31}$$

where the Ψ_{i,X_1}'s are some harmonic functions of (X_2, X_3) verifying on $\partial c_{X_1}(t)$ the following time-independent boundary conditions deduced from (30) :

$$\frac{\partial\Psi_{1,X_1}}{\partial\overline{n}_{X_1}} = (\overline{x}_{X_1} \times \overline{n}_{X_1}).t_1(X_1) \ , \ \frac{\partial\Psi_{\alpha,X_1}}{\partial\overline{n}_{X_1}} = (\overline{n}_{X_1}.t_\alpha)(X_1), \alpha = 2, 3. \tag{32}$$

Now if ρ_f is the fluid mass per unit of volume, the general expression for the kinetic energy T_f of the fluid contained in the control box $\mathcal{D}$ is given by :

$$T_f = \frac{1}{2}\int_{\mathcal{D}} \rho_f \nabla(\phi)^2 d\mathcal{D} = \frac{1}{2}\int_{\mathcal{D}} \rho_f(\nabla(\phi\nabla(\phi)) - \phi\Delta\phi)d\mathcal{D}. \tag{33}$$

Then from Stokes theorem and because ϕ is harmonic in $\mathcal{D}$, we find :

$$T_f = \frac{1}{2}\int_{\partial\mathcal{D}} \rho_f \phi \left(\frac{\partial \phi}{\partial n}\right) d\partial\mathcal{D}. \tag{34}$$

But the fluid being at rest at infinity and due to the approximation (28-30), (34) can be rewritten as :

$$T_f = \frac{1}{2}\int_0^1 \rho_f \left(\int_{\partial c_{X_1}} \overline{\phi}_{X_1} \left(\frac{\partial \overline{\phi}_{X_1}}{\partial \overline{n}_{X_1}}\right) d\partial c_{X_1}\right) dX_1 = \int_0^1 \mathfrak{T}_f \; dX_1, \tag{35}$$

where $\mathfrak{T}_f$ is the left invariant density of kinetic energy of the fluid stratified inside $\mathcal{D}$, which can be rewritten by inserting the Kirchhoff form (31) into (35), as :

$$\mathfrak{T}_f(\eta) = \frac{1}{2}\eta.(\mathbb{J}_f.\eta), \tag{36}$$

with $\mathbb{J}_f(X_1)$, the tensor of added (or "virtual") masses of the X_1 cross section which for an elliptic profile, can be detailed as follows :

$$\mathbb{J}_f = \begin{pmatrix} J_f & 0 \\ 0 & M_f \end{pmatrix}. \tag{37}$$

Finally, from complex planar potential flow theory and conform mapping, we have : $J_f = \rho_f(\pi/8)(a^2 - b^2)^2 E_1 \otimes E_1$, and $M_f = \rho_f \pi(b^2 E_2 \otimes E_2 + a^2 E_3 \otimes E_3)$, with $2a(X_1)$ and $2b(X_1)$ the length of the major and minor axes of the beam elliptic cross section c_{X_1} respectively. Lastly, thanks to the the slender-body assumption and the Kirchhoff potentials approach, we were able to reduce the configuration space of the fluid contained in $\mathcal{D}$ onto that of the beam defined by (2) as it is done in [25] for the discrete multi-body case.

4.3 Remark about the Large Amplitude E.B.T.

In the case when the fish body endures deformations of finite amplitudes, the previous stratification of the three dimensional flow in $\mathcal{D}$ cannot be achieved in all cases. In fact, due to the beam curvatures, the geometric planes s_{X_1} prolonging the beam cross sections c_{X_1} will intersect so forcing the fluid slices to mix together (as in the multi-body case of [25]). Be that as it may, the author of the L.A.E.B.T. neglects this phenomenon, which is assumed to occur sufficiently far from the body to have negligible effects on its dynamics. Nevertheless, this choice gives to the L.A.E.B.T. the heuristic character discussed at the end of section 2. Finally, contrary to the case of the E.B.T. which is funded on the previous kinematics, deduced from an expansion in perturbations of the slender (rigid) body theory, the L.A.E.B.T. is directly introduced through the basic fluid kinetics (36) (in fact the density of lateral impulses) which in the case of the planar swim studied by Lighthill reduces to $\mathfrak{T}_f = (1/2)mV_2^2$ (with $m = \rho_f \pi a^2$) [29], [10].

5 Generalisation of the Poincaré-Cosserat picture to the L.A.E.B.T.

The purpose of this section is to apply the Poincaré-Cosserat picture to the previous three-dimensional L.A.E.B.T.. For this, it is worth noting here that the context of section 3 differs from this now studied in two points. Firstly, the fluid kinetic energy has to be added to the body Lagrangian of (7), in order to define the Lagrangian of the total ("fluid" plus "body") material system contained at each instant in $\mathcal{D}$:

$$L = \int_0^1 \mathfrak{L} \; dX_1 = \int_0^1 \mathfrak{T}_b + \mathfrak{T}_f - \mathfrak{U}_b \; dX_1. \tag{38}$$

Secondly, due to the fluid flowing out of $\mathcal{D}$, the material system contained at each instant in the control box $\mathcal{D}$ is an "open material system." Hence, as this is usually the case for this type of systems [43], we wait for some new inertial terms (for instance modeling the ejection of matter through the control surface bounding the system) that do not appear in the case of usual "closed material systems" (like the beam alone for instance). As we will see in this section, in our case these new terms correspond to the "rate of change of momentum within $\mathcal{D}$ due to momentum transport across the plane π" of (1) here generalized to the three dimensional swim. Furthermore, they can be completely deduced from the fluid kinetic energy of (38) by using the following extension of the Hamilton principle (4) to the case of our stratified fluid flowing out of $\mathcal{D}$ (see B) :

$$\int_{t_1}^{t_2}\int_0^1 \delta(\mathfrak{T}_f+\mathfrak{T}_b-\mathfrak{U}_b)\,dX_1dt=\int_{t_1}^{t_2}\left(\delta W_{ext}-\left[\left(V_1\frac{\partial\mathfrak{T}_f}{\partial\eta}-\mathfrak{T}_f\begin{pmatrix}0\\E_1\end{pmatrix}\right).\delta\zeta\right]_0^1\right)dt, \tag{39}$$

where the boundary term of the r.h.s. is due to the relative motion of the two stratified media (the beam and the stratification of fluid slices), defined by (see B.1 in the appendix) :

$$\eta_f=\eta-V_1\xi, \tag{40}$$

with η_f, the twist of the fluid slice (which coincides with the geometric slice $s_{X_1}(t)$) prolonging c_{X_1} at the current time t.

5.1 Generalization of the Poincaré equations to the L.A.E.B.T.

Before developing (39) through variational calculus, one should point out that $\mathfrak{T}_f$, defined by (36,37), being mechanically related to the fluid, it should be a quadratic form of the fluid slice twists η_f rather than η. In fact this is actually the case since taking (12,13) and the sparse form of (37) into account, allows one to write :

$$\mathbb{J}_f.\xi=\mathbb{J}_f.\xi_d=0\ . \tag{41}$$

Hence, replacing η by (40) in (36), (41) does impose $\mathfrak{T}_f(\eta)=\mathfrak{T}_f(\eta_f)$. Furthermore, if taking $\mathfrak{T}_f$ as a function of η or η_f seems indifferent in (39), however, when developing (39), $\mathfrak{T}_f$ should be varied on the Reissner beam configuration space, i.e. with any $\delta\xi$ defined by (9.b). However, since from (40) we have : $(\delta\eta_f=\delta\eta-V_1\delta\xi-\xi\delta V_1)\neq\delta\eta$, it is necessary (as it will be confirmed at the end of this subsection) for the completeness of the variational calculus to take $\mathfrak{T}_f=\mathfrak{T}_f(\eta_f)$ in (39), and to write :

$$\delta\mathfrak{T}_f=\left(\frac{\partial\mathfrak{T}_f}{\partial\eta_f}\right).\delta\eta_f=\left(\frac{\partial\mathfrak{T}_f}{\partial\eta_f}\right).(D.\delta\eta-V_1\delta\xi), \tag{42}$$

where we introduced the tensor $D(\xi)=1-\xi\otimes(0^T,E_1^T)^T$ such that $D.\delta\eta=\delta\eta-\xi\delta V_1$ and where "1" here denotes the unit tensor of $\mathbb{R}^6\otimes\mathbb{R}^6$. Then, using (9) and the linearity of the co-adjoint map, we can write :

$$\delta\mathfrak{T}_f=\left(\frac{\partial\mathfrak{T}_f}{\partial\eta_f}\right).\left(D.\left(\frac{\partial\delta\zeta}{\partial t}+ad_{*\eta}(\delta\zeta)\right)-\left(V_1\frac{\partial\delta\zeta}{\partial X_1}+ad_{*\xi}(V_1\delta\zeta)\right)\right). \tag{43}$$

Now inserting (43) into the integral fluid contribution of (39), gives :

$$\int_{t_1}^{t_2}\int_0^1\delta\mathfrak{T}_f dX_1dt=I_1+I_2, \tag{44}$$

$$\text{with : } I_1 = \int_{t_1}^{t_2}\int_0^1 \left(\frac{\partial \mathfrak{T}_f}{\partial \eta_f}\right) \ . \ \left(D.\left(\frac{\partial \delta\zeta}{\partial t} + ad_{*\eta}(\delta\zeta)\right)\right) dX_1 dt = \tag{45}$$
$$\int_{t_1}^{t_2}\int_0^1 \delta\zeta.\left(-\frac{\partial}{\partial t}\left(D^T.\frac{\partial \mathfrak{T}_f}{\partial \eta_f}\right) + ad^*_\eta\left(D^T.\frac{\partial \mathfrak{T}_f}{\partial \eta_f}\right)\right) dX_1 dt,$$

$$\text{and : } I_2 = \int_{t_1}^{t_2}\int_0^1 \left(\frac{\partial \mathfrak{T}_f}{\partial \eta_f}\right).\left(-\frac{\partial \delta\zeta}{\partial X_1}V_1 - ad_{*\xi}(V_1\delta\zeta)\right) dX_1 dt = \tag{46}$$
$$\int_{t_1}^{t_2}\left(\left[\delta\zeta.\left(-V_1\frac{\partial \mathfrak{T}_f}{\partial \eta_f}\right)\right]_0^1 - \int_0^1 \delta\zeta.\left(\frac{\partial}{\partial X_1}\left(-V^1\frac{\partial \mathfrak{T}_f}{\partial \eta_f}\right) + V_1 ad^*_\xi\left(\frac{\partial \mathfrak{T}_f}{\partial \eta_f}\right)\right) dX_1\right) dt.$$

Now, in agreement with the subsection 3.4, because all the variational calculations are achieved (i.e. $\delta\zeta$ is in factor of all the contributions of I_1 and I_2), we can force again : $\xi = \xi_d$. Consequently from (41), we have : $\partial\mathfrak{T}_f/\partial\eta_f = \mathbb{J}_f.\eta_f = \mathbb{J}_f.(\eta - V_1\xi_d) = \mathbb{J}_f.\eta = \partial\mathfrak{T}_f/\partial\eta$, and $D^T(\xi_d).(\partial\mathfrak{T}_f/\partial\eta_f) = (1 - (0^T, E_1^T)^T \otimes \xi_d).(\mathbb{J}_f.\eta_f) = \mathbb{J}_f.\eta_f - 0 = (\partial\mathfrak{T}_f/\partial\eta_f)$, in (45,46). Then, taking these simplifications into account in (44) and (39), allows one to deduce the dynamics of all the matter contained in the control box $\mathcal{D}$ as :

$$\frac{\partial}{\partial t}\left(\frac{\partial(\mathfrak{T}_b + \mathfrak{T}_f)}{\partial \eta}\right) - ad^*_\eta\left(\frac{\partial(\mathfrak{T}_b + \mathfrak{T}_f)}{\partial \eta}\right) =$$
$$\frac{\partial}{\partial X_1}\left(\frac{\partial \mathfrak{U}_b}{\partial \xi} + V_1\frac{\partial \mathfrak{T}_f}{\partial \eta}\right) - ad^*_\xi\left(\frac{\partial \mathfrak{U}_b}{\partial \xi} + V_1\frac{\partial \mathfrak{T}_f}{\partial \eta}\right) + \overline{F}, \tag{47}$$

with the boundary conditions of the total system :

$$\left(\frac{\partial \mathfrak{U}_b}{\partial \xi}\right)(0) = \lambda(0) = -\left(\mathfrak{T}_f\begin{pmatrix} 0 \\ E_1 \end{pmatrix}\right)(0) + F_-, \tag{48}$$

$$\left(\frac{\partial \mathfrak{U}_b}{\partial \xi}\right)(1) = \lambda(1) = -\left(\mathfrak{T}_f\begin{pmatrix} 0 \\ E_1 \end{pmatrix}\right)(1) - F_+. \tag{49}$$

Furthermore, pre-multiplying each of the two rows of (47-49) by $R(X_1)$ allows one to obtain the dynamics of all the matter in $\mathcal{D}$ in the spatial setting :

– Field equations of the total system (fluid + body) :

$$\frac{\partial}{\partial t}\begin{pmatrix} \sigma_b + \sigma_f \\ p_b + p_f \end{pmatrix} + \begin{pmatrix} (\partial r/\partial t) \times p_f \\ 0 \end{pmatrix}$$
$$= \frac{\partial}{\partial X_1}\begin{pmatrix} c + V_1\sigma_f \\ n + V_1 p_f \end{pmatrix} + \begin{pmatrix} t_1 \times (n + V_1 p_f) \\ 0 \end{pmatrix} + \begin{pmatrix} \overline{c} \\ \overline{n} \end{pmatrix}. \tag{50}$$

– Boundary conditions of the total system :

$$\begin{pmatrix} c \\ n \end{pmatrix}(0) = \begin{pmatrix} 0 \\ -\mathfrak{T}_f t_1 \end{pmatrix}(0) + \begin{pmatrix} c_- \\ n_- \end{pmatrix}, \ \begin{pmatrix} c \\ n \end{pmatrix}(1) = \begin{pmatrix} 0 \\ -\mathfrak{T}_f t_1 \end{pmatrix}(1) - \begin{pmatrix} c_+ \\ n_+ \end{pmatrix}. \tag{51}$$

Before closing this section it is worth noting here, that for any $X_1 \in]0,1[$, the equations (50) state the balance of kinetic amounts of all the mater contained in the geometric strip bounded by the planes s_{X_1} and $s_{X_1+dX_1}$, both attached to the beam (see figure 4). Hence, this balance contains three types of terms : 1°) the usual terms of the beam alone (23), 2°) the terms modeling the proper time-rate of changes of the fluid kinetic amounts (they have the same form as the previous ones with the fluid kinetic amounts replacing the body ones), 3°) those modeling the

time-rate of change of the fluid kinetic amounts of the strip due to the fact that the fluid slices sweep past the body ones (these are the terms containing V_1). Finally, let us remark that if (39) is computed by taking $\mathfrak{T}_f(\eta)$ instead of $\mathfrak{T}_f(\eta_f)$, all the terms of the third type disappear although they should not. Lastly, following [16], the terms containing $\mathfrak{T}_f$ in (51) can be interpreted as the resultant forces exerted by the fluid outside $\mathcal{D}$ across $s_{X_1=0}$ and $s_{X_1=1} = \pi$.

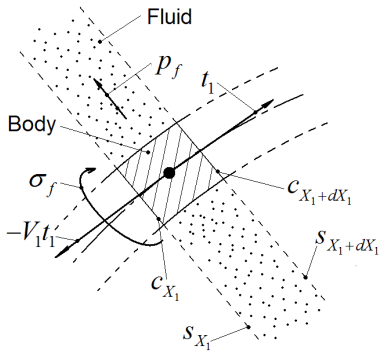

FIG. 4 – The kinetic amounts of all mater contained in the geometric strip bounded by the planes s_{X_1} and $s_{X_1+dX_1}$.

6 External (head) dynamics

Devoted to the locomotion control and the study of swimming gaits, the algorithm of [1] needs to derive the dynamics of the eel on the principal fiber bundle $SE(3) \times \mathbb{S}$ where the fiber $SE(3)$ stands for the head configuration space i.e. the set of all the $g(X_1 = 0) \triangleq g_o$'s, while the shape space $\mathbb{S}$, is here defined by the functional set of curves in the Lie algebra $so(3)$:

$$\mathbb{S} \triangleq \{K : X_1 \in [0,1] \mapsto K(X_1) = K_2 E_2 + K_3 E_3 \in so(3)\}. \tag{52}$$

In fact, when the eel swims, the internal actuators impose the constraint (12.a) at each instant and the eel propels its head (external d.o.f.) by reaction due to the hydrodynamic forces applied by the fluid on its body. This dynamic model, formally denoted G_{ext} in (27), is derived from the weak form of virtual work balance here applied to all the mater in $\mathcal{D}$ and consistent with the strong form (50-51) :

$$\begin{aligned} &\int_0^1 \delta\nu . \left(\frac{\partial}{\partial t} \begin{pmatrix} \sigma_b + \sigma_f \\ p_b + p_f \end{pmatrix} - \frac{\partial}{\partial X_1} \begin{pmatrix} V_1 \sigma_f \\ V_1 p_f \end{pmatrix} - \begin{pmatrix} t_1 \times V_1 p_f \\ 0 \end{pmatrix} \right) dX_1 \\ &= \int_0^1 \left(\delta\xi . \lambda + \delta\nu . \begin{pmatrix} \overline{c} \\ \overline{n} \end{pmatrix} \right) dX_1 - \left[\delta\nu . \begin{pmatrix} 0 \\ \mathfrak{T}_f t_1 \end{pmatrix} \right]_0^1 + \delta\nu(0) . \begin{pmatrix} c_- \\ n_- \end{pmatrix} - \delta\nu(1) . \begin{pmatrix} c_+ \\ n_+ \end{pmatrix}, \end{aligned} \tag{53}$$

where $\delta\nu = \delta g g^{-1}$ denote any spatial field of virtual twist applied along the beam. Then, let us introduce the two maps : $Ad_{g*} : se(3) \to se(3)$ and $Ad_g^* : se(3)^* \to se(3)^*$ such that :

$$Ad_{g*} = \begin{pmatrix} 1 & 0 \\ -\widehat{r} & 1 \end{pmatrix}, \; Ad_g^* = \begin{pmatrix} 1 & \widehat{r} \\ 0 & 1 \end{pmatrix}, \tag{54}$$

where 1 denotes the identity tensor of $\mathbb{R}^3 \otimes \mathbb{R}^3$, and $g \in SE(3)$ is given by (3). Now, in order to derive the head dynamics, we just have to take in (53) a virtual displacement field $\delta\nu$ defined by :

$$\delta\nu(X_1) = Ad_{h(X_1)*}.\delta\nu_o, \tag{55}$$

with $h(X_1) = g_o^{-1}g(X_1)$, and $\delta\nu_o = (\delta g g^{-1})(0)$ denoting the configuration of the X_1-cross section with respect to the head frame and the head spatial virtual twist respectively. It is worth noting here, that with this restriction, the "virtual motion" defined by (55) is a rigid one imposed on the eel (through its head) while it is in its current frozen internal configuration. Consequently, with such a virtual field, the virtual work of internal wrenches "$\delta\mathfrak{U}_b = \int_0^1 \delta\xi.\lambda\ dX_1$" is necessary zero, and we can rewrite (53) as :

$$\begin{aligned}&\delta\nu_o.\int_0^1 Ad^*_{h(X_1)}.\left(\frac{\partial}{\partial t}\begin{pmatrix}\sigma_b+\sigma_f\\ p_b+p_f\end{pmatrix}-\frac{\partial}{\partial X_1}\begin{pmatrix}V_1\sigma_f\\ V_1p_f\end{pmatrix}-\begin{pmatrix}t_1\times V_1p_f\\ 0\end{pmatrix}\right)dX_1 \\ &=\delta\nu_o.\left\{\int_0^1 Ad^*_{h(X_1)}.\begin{pmatrix}\overline{c}\\ \overline{n}\end{pmatrix}dX_1-\left[Ad^*_{h(X_1)}.\begin{pmatrix}0\\ \mathfrak{T}_f t_1\end{pmatrix}\right]_0^1+\begin{pmatrix}c_-\\ n_-\end{pmatrix}-Ad^*_{h(1)}.\begin{pmatrix}c_+\\ n_+\end{pmatrix}\right\}.\end{aligned} \tag{56}$$

Now, let us consider the two last terms of the l.h.s. of (56), we have :

$$\begin{aligned}&\int_0^1 Ad^*_h.\left[\frac{\partial}{\partial X_1}\begin{pmatrix}V_1\sigma_f\\ V_1p_f\end{pmatrix}+\begin{pmatrix}V_1t_1\times p_f\\ 0\end{pmatrix}\right]\quad dX_1 \\ &\qquad=\int_0^1\frac{\partial}{\partial X_1}\left[Ad^*_h.\begin{pmatrix}V_1\sigma_f\\ V_1p_f\end{pmatrix}\right]\quad+\begin{pmatrix}V_1t_1\times p_f\\ 0\end{pmatrix}-\frac{\partial Ad^*_h}{\partial X_1}.\begin{pmatrix}V_1\sigma_f\\ V_1p_f\end{pmatrix}dX_1.\end{aligned} \tag{57}$$

Hence, because :

$$\begin{aligned}&\int_0^1\begin{pmatrix}V_1t_1\times p_f\\ 0\end{pmatrix}\ -\ \frac{\partial Ad^*_h}{\partial X_1}.\begin{pmatrix}V_1\sigma_f\\ V_1p_f\end{pmatrix}dX_1= \\ &\qquad\int_0^1\begin{pmatrix}V_1t_1\times p_f\\ 0\end{pmatrix}-\begin{pmatrix}0&\widehat{t}_1\\ 0&0\end{pmatrix}.\begin{pmatrix}V_1\sigma_f\\ V_1p_f\end{pmatrix}dX_1=0\ ,\end{aligned} \tag{58}$$

we can rewrite (57) as :

$$\begin{aligned}\int_0^1 Ad^*_h.\left[\frac{\partial}{\partial X_1}\begin{pmatrix}V_1\sigma_f\\ V_1p_f\end{pmatrix}+\begin{pmatrix}V_1t_1\times p_f\\ 0\end{pmatrix}\right]dX_1\ &=\ \int_0^1\frac{\partial}{\partial X_1}\left[Ad^*_h.\begin{pmatrix}V_1\sigma_f\\ V_1p_f\end{pmatrix}\right]dX_1 \\ &=\left(V_1Ad^*_h\begin{pmatrix}\sigma_f\\ p_f\end{pmatrix}\right)(1)\ -\ V_1(0)\begin{pmatrix}\sigma_f(0)\\ p_f(0)\end{pmatrix}.\end{aligned} \tag{59}$$

Finally, inserting (59) into (56), gives with $p = p_b + p_f$ and $\sigma = \sigma_b + \sigma_f$:

$$\begin{aligned}\int_0^1\begin{pmatrix}\partial\sigma/\partial t+(\partial r/\partial t)\times p_f+r\times(\partial p/\partial t)\\ \partial p/\partial t\end{pmatrix}dX_1\ &=\ \left[Ad^*_h\begin{pmatrix}V_1\sigma_f\\ V_1p_f-\mathfrak{T}_f t_1\end{pmatrix}\right]_0^1+ \\ &+\int_0^1 Ad^*_h\begin{pmatrix}\overline{c}\\ \overline{n}\end{pmatrix}dX_1\ +\ \begin{pmatrix}\overline{c}_-\\ \overline{n}_-\end{pmatrix}-Ad^*_{h(1)}\begin{pmatrix}c_+\\ n_+\end{pmatrix}.\end{aligned} \tag{60}$$

Now, let us remark that because the eel's cross section $c_{X_1=0}$ reduces to a single particle, its added mass tensor is equal to zero. Hence, splitting the fluid and body kinetic amounts in (60) and removing the external loads which are not present in the Lighthill reactive modeling, give

the following expression of the wrench f_h (w.r.t. the origin of space), of the hydrodynamic forces applied onto the eel :

$$f_h = -\frac{\partial}{\partial t}\int_0^1 \begin{pmatrix} \sigma_f + r \times p_f \\ p_f \end{pmatrix} dX_1 + V_1(1) \begin{pmatrix} \sigma_f + r \times p_f \\ p_f \end{pmatrix}(1) - \begin{pmatrix} r \times \mathfrak{T}_f t_1 \\ \mathfrak{T}_f t_1 \end{pmatrix}(1). \tag{61}$$

Finally, in the case of the planar swim in (e_1, e_2), we have $V_3 = \Omega_1 = 0$ and so : $\sigma_f = 0, p_f = mV_2t_2$ and $\mathfrak{T}_f = (1/2)mV_2^2$. Then taking these considerations into account in (61), gives the Lighthill Large Amplitude E.B.T. model of (1), whose (61) is nothing but the three dimensional generalization.

7 Simulations

7.1 Principle of the algorithm

Following the remarks of subsection 3.3, the principle of the algorithm is the following. It is structured by two spatial integration loops computing G_{ext} and G_{int} respectively, and both included in a global time loop. The inputs are the current head state (g_o, μ_o) and the internal curvature time law K_d. The first space integration loop G_{ext} starts by forward integrating (from the head to the tail) the beam kinematics (configuration, velocity). Then making the head accelerations explicitly appear in (60) allows one to write G_{ext} as $G_{ext} = \mathbb{I}_o^{-1}.\mathbb{F}_o$ where the inertia tensor $\mathbb{I}_o$ and the wrench $\mathbb{F}_o$ are computed through a forward space integration included in the first space loop (see [1] for more details). Finally, the first space-loop ends and (27) is time-integrated in order to update the head state. Then, G_{int} starts by computing the beam accelerations by a forward space-integration initialized by the head acceleration previously computed. Then, forward space integrating (50) gives the internal forces n and finally the control torque C, which, once completed with the head accelerations $\dot{\mu}_o$, are the outputs of the algorithm at the current time. Finally, the time is updated and the algorithm resumes.

7.2 A numerical example

In this section, we report a numerical example obtained with the algorithm of subsection 7.1. The concerned result is a "three dimensional rising and falling gait". For more details about numerical aspects we invite the reader to consult [18] where a complete set of planar gaits is also tested and compared to Navier-Stokes simulations with many gaits parameters. The algorithm was implemented in C++ on a workstation with a Pentium IV (3.2 GHz with 1Go of Ram). The integrations of space and time loops are achieved with a fourth order RK method. All the tests presented below work between "0.2 and 0.7 times the real time" and are thus compatible with on-line computation.

7.2.1 Geometric description of the eel-like robot and corrections of the L.A.E.B.T.

The straight reference geometry of the robot is drawn in figure 5. Its total length l is one meter. Its material is assumed to be homogeneous with a "mass/volume" ratio equal to that of water to ensure a buoyancy neutrality (the mass is $1.94Kg$). The shape is first defined as a cylinder of diameter $D = 0.1m$ for any $X_1 \in [0.05, 1]$. This cylinder is covered with an half-ellipsoid between $X_1 = 0$ and $X_1 = 0.05$. Next, this shape is deformed as follows. For any cross section, the minor axis (along E_2) is multiplied by $A(X_1)$, and its major axis (along E_3) by

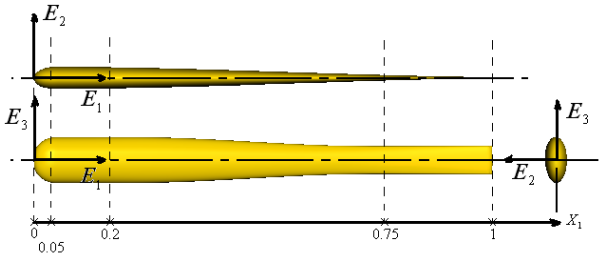

FIG. 5 – Geometry of the Body.

$B(X_1)$, where A and B are two functions defined by :

$$\begin{aligned} A(X_1) &= -\frac{1}{6}\left[\sin\left(\pi X_1 - \frac{\pi}{2}\right) + 1\right] - \frac{X_1^2}{8} + \frac{1}{2} \text{ , for : } 0 \leq X_1 < 1, \\ B(X_1) &= 1 \text{ , for : } 0 \leq X_1 < \frac{1}{5}, B(X_1) = \frac{3}{5} \text{ , for : } \frac{3}{4} \leq X_1 < 1, \\ B(\tilde{X_1}) &= 1 - \frac{\sin(\pi\tilde{X_1} - \pi/2) + 1}{5} \text{ , for : } \frac{1}{5} \leq X_1 < \frac{3}{4} \text{ , with } \tilde{X_1} = \frac{20X_1 - 4}{11}. \end{aligned}$$

As far as the contact model is concerned, the reactive component is fixed by the added mass tensor of subsection 4.2 with the above geometry which allows one to deduce the minor and major axes length $2a(X_1)$ and $2b(X_1)$ of any cross section c_{X_1}. As proposed in [18], this model is firstly improved with the following axial corrections which model the resistive and reactive forces applied onto the rounded nose neglected by the slender body assumption : $c_- = 0$, $n_- = n_{reac-} + n_{res-}$, with : $n_{reac-} = -m_o((t_1.(\partial^2 r/\partial t^2))t_1)(0)$, and $n_{res-} = -(1/2)\rho_f k_o(V_1|V_1|t_1)(0)$. Secondly, the effects of the fluid viscosity on the body are modeled by the following slice by slice resistive model : $\forall X_1 \in]0,1[$: $\overline{n}(X_1) = \overline{n}_{res}(X_1)$, $\overline{c}(X_1) = \overline{c}_{res}(X_1)$, where : $\overline{c}_{res} = (-1/2)\rho_f k_4 \Omega_1|\Omega_1|t_1$, $\overline{n}_{res} = (-1/2)\rho_f \sum_{i=1}^{i=3} k_i V_i|V_i|t_i$; while no force is applied onto the trailing edge except the inertial ones of the reactive model, i.e. $n_+ = 0$, $c_+ = 0$. Thirdly, in agreement with the standard uses of naval engineering [44, 45, 46], we took the following expressions : $m_o = \rho_f \pi k a_o b_o c_o$, $k_o = \pi c_p a_o b_o$, $k_4 = c_1\pi(a^2 - b^2)^2$, $k_1 = c_f P$ (where $P \simeq \pi/2((3/2)(a+b) - \sqrt{ab})$ stands for the elliptic cross section perimeter), $k_2 = 2c_2 a$, $k_3 = 2c_3 b$. Lastly, according to the robot geometry and "a trial and error based strategy" using Navier-Stokes simulations [18], we took the following values (fixed once and for all in all the simulations) : $a_0 = 0.025\,m$, $b_0 = c_0 = 0.05\,m$, $k = 0.32$, $c_p = 0.036$, $c_1 = 1$, $c_2 = 1.98$ and $c_3 = 1$. Finally c_f is defined as follows in order to take into account the transition phenomena in the boundary layer (laminar flow to turbulent flow) : $c_f = 0.664/Re^{0.5}$, for : $Re \leq 8.10^4$,$c_f = 0.059/Re^{1/5}$, for : $Re > 8.10^4$; where we introduced the local axial Reynolds number $Re(X_1) = (V_1 X_1)/\nu$ and ν the kinematic viscosity of water.

7.2.2 Example : three-dimensional rising and falling gait

The goal of this example is to achieve a falling gait or "submergence" from one given altitude to another (see fig.6). This is accomplished with the following "pitch-yaw curvature" law :

$$K_d(t, X_1) = K_2(t, X_1)E_2 + K_3(t, X_1)E_3, \tag{62}$$

where we adopt the following yaw-curvature law :

$$K_3(t, X_1) = f_r(t, 0, T)K_{f3}(t, X_1), \tag{63}$$

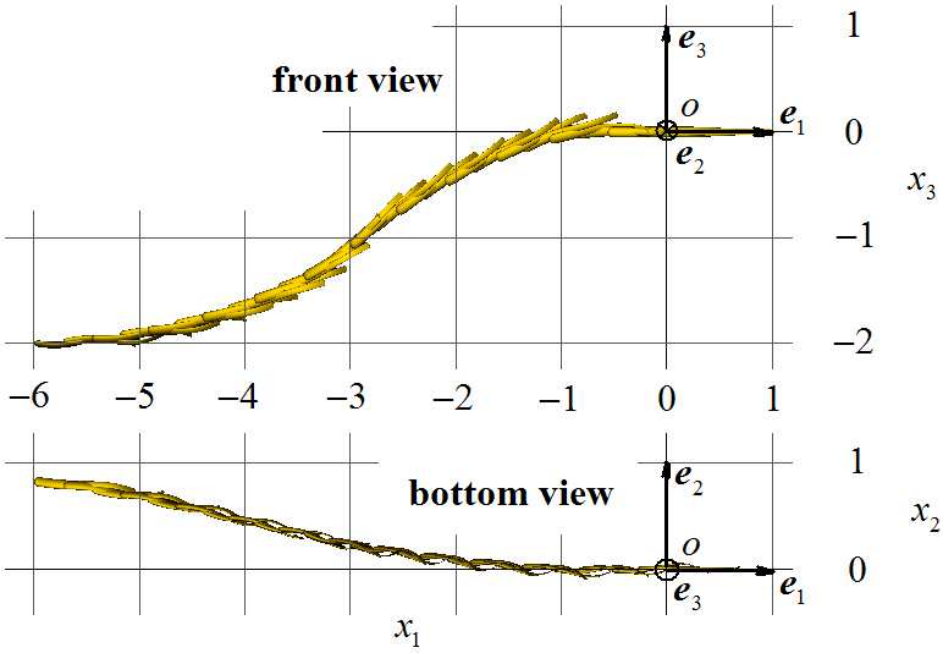

FIG. 6 – Body configurations for the falling gait ($2fps$).

with $f_r(.,t_i,t_f)$, a sinusoid ramp defined by :

$$f_r(t,t_i,t_f) = 0 \quad \text{, for :} \quad 0 \leq t < t_i,$$
$$f_r(t,t_i,t_f) = \frac{t-t_i}{t_f-t_i} - \frac{1}{2\pi}\sin\left(2\pi\frac{t-t_i}{t_f-t_i}\right) \quad \text{, for :} \quad t_i \leq t < t_f,$$
$$f_r(t,t_i,t_f) = 1 \quad \text{, for :} \quad t \geq t_f, \tag{64}$$

which has null first and second order derivatives at the commutation instants thereby guaranteeing smooth time transitions, while K_{f3} (with f for "forward"), is the backward sinusoidal wave (traveling from the head to the tail) of the nominal "straight-line swim" as it has been extensively studied in the zoological literature [47, 48, 49], i.e. :

$$K_{f3}(t,X_1) = f_a(X_1)\sin\left[2\pi\left(\frac{X_1}{\lambda}-\frac{t}{T}\right)\right] \text{ , with } \quad f_a(X_1) = a_2X_1^2 + a_1X_1 + a_0, \tag{65}$$

where : λ is the wave length, T is its period and a_0, a_1, a_2 are the coefficients of the amplitude modulation polynomial function f_a. Finally, we also took the following pitch-curvature law :

$$K_2(t,X_1) = K_{c2}\ \gamma(t), \tag{66}$$

with K_{c2} a constant component, and $\gamma(t) = f_r(t,t_1,t_2)$, for : $t < t_2$, $\gamma(t) = 1 - f_r(t,t_2,t_3)$, for : $t_2 \leq t < t_4$, $\gamma(t) = -f_r(t,t_4,t_5)$, for : $t_4 \leq t < t_5$, and $\gamma(t) = f_r(t,t_5,t_6) - 1$, for : $t \geq t_5$. Finally all the following results were obtained with the strain law (62) and the following parameters : $\lambda = 1m$, $T = 1s$, $a_2 = 2rad.m^{-3}$, $a_1 = 0.5rad.m^{-2}$ and $a_0 = 1rad.m^{-1}$, $K_{c2} = 0.5rad.m^{-1}$, $t_1 = 1s$, $t_2 = 2s$, $t_3 = 3s$, $t_4 = 6s$, $t_5 = 7s$ and $t_6 = 8s$.

On Figure 7 the spatial profiles are plotted (along the eel backbone) of the internal axial force N_1 and those of the two control torques C_2 and C_3. On fig.8, the same internal stresses are plotted but with respect to the time and at a point located at the half of the eel length. Lastly, fig.9 shows the time evolution of the axial head velocity and of its angular roll one. While the roll dynamics play no role in the definition of the locomotion gaits, they are very influential on

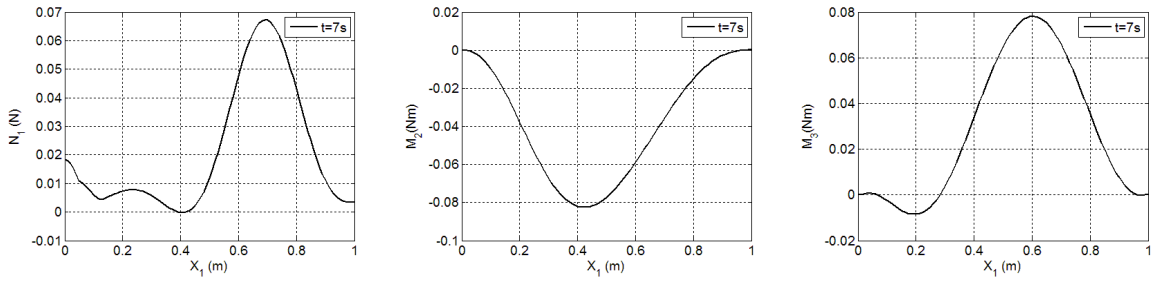

(a) N_1 at $t = 7s$. (b) C_2 at $t = 7s$. (c) C_3 at $t = 7s$.

FIG. 7 – "X_1 profile" of internal force N_1, and internal torques C_2 and C_3 at $t = 7s$ for the falling gait.

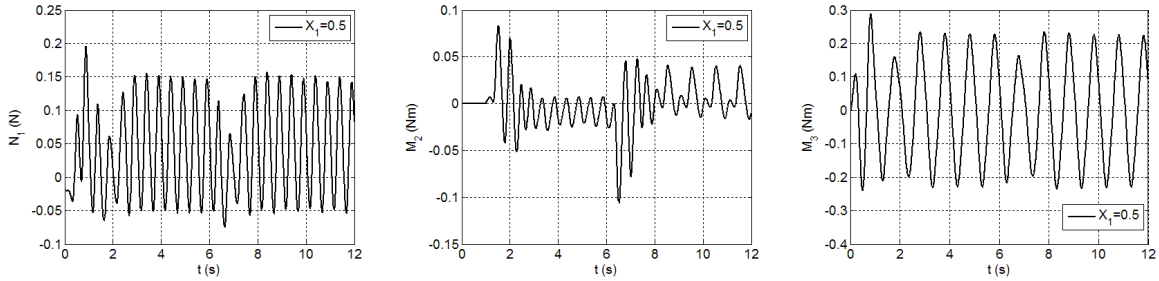

(a) N_1 at $X_1 = 0.5m$. (b) C_2 at $X_1 = 0.5m$. (c) C_3 at $X_1 = 0.5m$.

FIG. 8 – "t profile" of internal force N_1, and internal torques C_2 and C_3 at $X_1 = 0.5m$ for the falling gait.

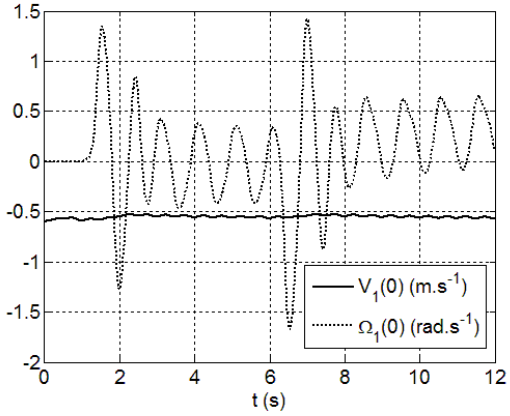

FIG. 9 – Time evolution of $V_1(0)$ and $\Omega_1(0)$ for the falling gait.

their control. For instance, in the case of the falling gait, they break the symmetry of the yaw dynamics and produce the deviation of fig.6. Thus, the roll dynamics will imperatively require a stabilization control based on the use of pectoral fins [50].

8 Conclusion

This article deals with the dynamic modeling of the anguilliform swim of elongated fishes. Devoted to the on-line control of an eel-like robot capable of swimming in the three dimensions,

the proposed solution is entirely analytic and once coupled to an algorithm recently proposed in [1], it works in a fraction of the real-time. The model is a generalization of the Large Amplitude Elongated Body Theory of Lighthill to the case of the three-dimensional swim. Furthermore, contrary to the Lighthill result, the swim is self-propelled and the internal body dynamics are also investigated. In order to derive this model, the article proposes to use a geometric framework due to Poincaré and here applied to a one dimensional Cosserat medium. Such media were extensively studied by J.C. Simo [30, 51] in the context of his "Geometrically-Exact" theory of finite elements. Because, this picture is originally restricted to the fish body, the article also extends the Poincaré equations from a standard Cosserat medium to a stratified fluid contained in a control volume laterally surrounding the fish body. This last extension is based on the Lighthill theory of anguilliform swim itself originally founded on the Slender Body Theory of aeronautics. Moreover, it uses a generalization of the Hamilton principle, also derived for this article, to a material open system. In our case, the open system is assimilated to the stratified fluid contained at each instant in the control volume which moves with the body. Once this generalized Hamilton principle obtained, its application gives the waited for reactive model of the three-dimensional anguilliform swim. Furthermore, like any Lagrangian based modeling, all the nonlinear dynamics forces are derived from the system Lagrangian and a "blind" variation calculus. This advantage is crucial here because of the "complexity" of fluid-structure interactions. Finally, while being sufficiently fast for on-line control, the model is sufficiently accurate too. In fact, comparisons with a Navier-Stokes solver for several gaits show discrepancies inferior to ten per-cents [18].

A Proof of the Cosserat beam equations ((10),(11))

The purpose of this appendix is to compute the field equations (10) and boundary conditions (11) by starting from the extended Hamilton principle (4), that we now restate for a left invariant density of Lagrangian of the form (7) and, with as external loads, a wrench density field $\overline{F}$ and the two punctual wrenches F_- and F_+, both applied onto the two tips of the beam :

$$\delta \int_{t_1}^{t_2} \int_0^1 \mathfrak{T}_b(\eta) - \mathfrak{U}_b(\xi) dX_1 dt = \int_{t_1}^{t_2} \int_0^1 \overline{F}.\delta\zeta dX_1 + F_-.\delta\zeta(0) + F_+.\delta\zeta(1) dt. \tag{67}$$

Because the variation δ is achieved while the time t is maintained fixed, we can first rewrite (67) as :

$$\int_{t_1}^{t_2} \left(\int_0^1 \delta\mathfrak{T}_b - \delta\mathfrak{U}_b \ - \delta\zeta.\overline{F} dX_1 - F_-.\delta\zeta(0) - F_+.\delta\zeta(1) \right) dt = 0, \tag{68}$$

where we have :

$$\int_{t_1}^{t_2} \int_0^1 \delta\mathfrak{T}_b - \delta\mathfrak{U}_b \ dX_1 dt = \int_{t_1}^{t_2} \int_0^1 \frac{\partial \mathfrak{T}_b}{\partial \eta}\delta\eta - \frac{\partial \mathfrak{U}_b}{\partial \xi}\delta\xi \ dX_1 dt. \tag{69}$$

Then, inserting (9) into (69), and integrating by part with respect to the time and space variables, gives, the two end times t_1 and t_2 being maintained fixed :

$$\begin{aligned} 0 = \int_{t_1}^{t_2} \int_0^1 \delta\zeta. \quad & \left(-\frac{\partial}{\partial t}\left(\frac{\partial \mathfrak{T}_b}{\partial \eta}\right) + ad^*_\eta\left(\frac{\partial \mathfrak{T}_b}{\partial \eta}\right) - \overline{F} \right) dX_1 dt - \\ & \int_{t_1}^{t_2} \left[\delta\zeta(1)\left(\frac{\partial \mathfrak{U}_b}{\partial \xi}(1) + F_+\right) - \delta\zeta(0)\left(\frac{\partial \mathfrak{U}_b}{\partial \xi}(0) - F_-\right) \right] dt \\ & - \int_{t_1}^{t_2} \int_0^1 \delta\zeta.\left(-\frac{\partial}{\partial X_1}\left(\frac{\partial \mathfrak{U}_b}{\partial \xi}\right) + ad^*_\xi\left(\frac{\partial \mathfrak{U}_b}{\partial \xi}\right) \ \right) dX_1 dt, \end{aligned} \tag{70}$$

which has to be verified for any $\delta\zeta$ so proving (10) and (11) when we insert in them a Lagrangian density of the form (7).

B Proof of the statement (39)

The purpose of this appendix is to prove (39). This extension of the Hamilton principle requires the use of a one-dimensional version of the transport Reynolds theorem (subsection B.2) devoted to the kinematics of two stratified media moving axially, the one w.r.t. the other (B.1). Once these results are in hand, the variational principle is deduced from the D'Alembert principle of virtual works here revisited for our particular case (subsection B.3). Finally, the appendix ends with (B.4) where (39) is stated.

B.1 More about kinematics

The purpose of what follows is to give more insight about the kinematics of the beam with respect to the fluid. Let us first introduce the particular derivative $d./dt$ which follows a fluid slice. If $d./dt$ is applied to a given function f, mechanically related to the stratified fluid state, but parameterized by the beam base variables (X_1, t), we have :

$$\frac{df}{dt}(X_1,t) = \frac{\partial f}{\partial t}(X_1,t) + \left(\frac{\partial f}{\partial X_1}\frac{dX_1}{dt}\right)(X_1,t), \tag{71}$$

where $dX_1/dt = -V_1(X_1,t)$ is the axial velocity of the X_1- beam cross section measured by an observer attached to the fluid slice which prolongs the beam cross section to $\mathcal{D}$ at the current time t. Now applying (71) to $g(X_1,t)$, gives (40), i.e. the twist of the fluid slice which prolongs the body slice c_{X_1} at the current time t. Corresponding to "$\partial./\partial t$" and "$d./dt$", we introduce two "variations", respectively denoted "$\delta.$" and "$\Delta.$". The first one (δ) is the variation related to the beam configuration space as already defined in the section 3, while the second one (Δ), follows the fluid slices, and as such can be named "particular variation". It is defined by replacing the time t in (71) by a variation parameter $\varepsilon \in \mathbb{R}$. Thus :

$$\Delta f = \delta f - \frac{\partial f}{\partial X_1}\delta\zeta_4, \tag{72}$$

where "$\delta\zeta_4 = \delta\zeta.(0^T, E_1^T)^T$", is the axial component of the virtual displacement applied to the X_1 body cross section.

B.2 One dimensional Reynolds transport theorem

Once these definitions introduced, a one dimensional version of the Reynolds transport theorem can be deduced of :

$$\frac{d}{dt}\int_0^1 f(X_1,t)\; dX_1 = \int_0^1 \frac{df}{dt}\; dX_1 + f\frac{d}{dt}(dX_1), \tag{73}$$

where because the space of cross sections moves with respect to the space of fluid slices, we do not have $d(dX_1)/dt = 0$ but rather : $d(dX_1)/dt = d(dX_1/dt) = (\partial(dX_1/dt)/\partial X_1)dX_1$. Furthermore, since we also have $dX_1/dt = -V_1$, we can rewrite (73), thanks to (71) as :

$$\frac{d}{dt}\int_0^1 f(X_1,t)\; dX_1 = \int_0^1 \left(\frac{\partial f}{\partial t} - \frac{\partial f}{\partial X_1}V_1 - f\frac{\partial V_1}{\partial X_1}\right) dX_1. \tag{74}$$

And we finally find :

$$\frac{d}{dt}\int_0^1 f\ dX_1 = \frac{\partial}{\partial t}\int_0^1 f\ dX_1\ - [fV_1]_0^1. \tag{75}$$

Finally (75) is merely a one-dimensional version of the Reynolds Transport theorem [41], where the boundary term stands for the flow of f outside of $\mathcal{D}$ after its stratification.

B.3 Coming back to the principle of virtual works

The purpose of this appendix is to prove that for any one-dimensional Cosserat medium $\mathcal{S}$ of Lagrangian $L = T - U = \int_0^1 \mathfrak{T} - \mathfrak{U}\ dX_1$ with $\mathfrak{L} = \mathfrak{T} - \mathfrak{U}$ having the reduced form (14), we have :

$$\delta L = \frac{\partial}{\partial t}\int_0^1 \left(\frac{\partial \mathfrak{T}}{\partial \eta}\right).\delta\zeta dX_1 + \delta W_{ext}, \tag{76}$$

where "δW_{ext}" is still the virtual work of the external load. For this, let us start from the D'Alembert principle of virtual works applied to $\mathcal{S}$:

$$\delta W_{acc} = \int_0^1 \left(\frac{\partial}{\partial t}\left(\frac{\partial \mathfrak{T}}{\partial \eta}\right) - ad^*_\eta\left(\frac{\partial \mathfrak{T}}{\partial \eta}\right)\right).\delta\zeta dX_1 = -\delta U - \delta W_{ext}, \tag{77}$$

where "δW_{acc}" and "$-\delta U$" are respectively the virtual works of the acceleration amounts, and this of the internal forces which are assumed to be conservative.

Then, let us remark that we also have :

$$\delta W_{acc} = \frac{\partial}{\partial t}\int_0^1 \left(\frac{\partial \mathfrak{T}}{\partial \eta}\right).\delta\zeta dX_1 - \int_0^1 ad^*_\eta\left(\frac{\partial \mathfrak{T}}{\partial \eta}\right).\delta\zeta + \left(\frac{\partial \mathfrak{T}}{\partial \eta}.\frac{\partial \delta\zeta}{\partial t}\right) dX_1. \tag{78}$$

Thus, inserting (9) into (78), gives :

$$\delta W_{acc} = \frac{\partial}{\partial t}\int_0^1 \left(\frac{\partial \mathfrak{T}}{\partial \eta}\right).\delta\zeta dX_1 - \delta T + \int_0^1 ad^*_\eta\left(\frac{\partial \mathfrak{T}}{\partial \eta}\right).\delta\zeta - ad_{\eta,*}\left(\delta\zeta\right).\frac{\partial \mathfrak{T}}{\partial \eta} dX_1. \tag{79}$$

But by the definition of the co-adjoint map, we can rewrite (77) as :

$$\delta W_{acc} = \frac{\partial}{\partial t}\int_0^1 \left(\frac{\partial \mathfrak{T}}{\partial \eta}\right).\delta\zeta dX_1 = \delta(T - U) - \delta W_{ext}, \tag{80}$$

and (80) does allow one to state (76). Finally, let us remark that in all the above computations $\delta.$ is a Lagrangian variation, i.e. it follows the cross sections along their virtual motion while X_1 plays the role of a continuous label.

B.4 Proof of (39)

Now let us consider the Cosserat medium $\mathcal{S}$ constituted by the beam (of Lagrangian $L_b = \int_0^1 \mathfrak{T}_b - \mathfrak{U}_b\ dX_1$) and the stratified fluid in $\mathcal{D}$ (of Lagrangian $L_f = T_f = \int_0^1 \mathfrak{T}_f\ dX_1$). From the concluding remark of the previous subsection, let us apply (76) to $\mathcal{S}$ with $(\delta., \partial./\partial t)$ for the beam, and $(\Delta., d./dt)$ for the fluid, we find :

$$\delta L_b + \Delta T_f = \frac{\partial}{\partial t}\int_0^1 \left(\frac{\partial \mathfrak{T}_b}{\partial \eta}\right).\delta\zeta dX_1 + \frac{d}{dt}\int_0^1 \left(\frac{\partial \mathfrak{T}_f}{\partial \eta}\right).\Delta\zeta dX_1 + \delta W_{ext}, \tag{81}$$

where δW_{ext} is still given by (67). Then let us apply to the fluid term of the r.h.s. of (81) the Reynolds theorem (75) with $d./dt$ and $f = (\partial\mathfrak{T}_f/\partial\eta).\Delta\zeta$. We find, after time integration on $[t_1, t_2]$ with $\delta\zeta(t_1) = \delta\zeta(t_2) = 0$:

$$\int_{t_1}^{t_2} \delta L_b + \left(\Delta\int_0^1 \mathfrak{T}_f \; dX_1\right) dt = \int_{t_1}^{t_2} \delta W_{ext} - \left[V_1 \frac{\partial \mathfrak{T}_f}{\partial \eta}.\Delta\zeta\right]_0^1 dt, \tag{82}$$

where we used the fact that from (72) applied to g, we have : $\Delta\zeta = \delta\zeta - \delta\zeta_4\xi$, and so $\delta\zeta(t_1) = \delta\zeta(t_2) = 0 \Rightarrow \Delta\zeta(t_1) = \Delta\zeta(t_2) = 0$. Furthermore, applying now (75) to the l.h.s. of (82), i.e. with "$\Delta.$" instead of "$d./dt$", and $f = \mathfrak{T}_f$, we find, by remarking from (72) that $\Delta X_1 = -\delta\zeta_4 = -\delta\zeta.(0^T, E_1^T)^T$, the following new form of (4) :

$$\int_{t_1}^{t_2} \delta L_b + \left(\int_0^1 \delta\mathfrak{T}_f dX_1 + \left[V_1 \frac{\partial \mathfrak{T}_f}{\partial \eta}.\Delta\zeta - \mathfrak{T}_f \begin{pmatrix} 0 \\ E_1 \end{pmatrix}.\delta\zeta\right]_0^1\right) dt = \int_{t_1}^{t_2} \delta W_{ext} dt. \tag{83}$$

But, introducing $\Delta\zeta = \delta\zeta - \delta\zeta_4\xi$, into the boundary term of (83), we obtain :

$$\begin{aligned} &\int_{t_1}^{t_2} (\delta W_{ext} - \delta L_b) dt = \\ &\int_{t_1}^{t_2} \left(\int_0^1 \delta\mathfrak{T}_f dX_1 + \left[\left(V_1 \frac{\partial \mathfrak{T}_f}{\partial \eta} - \left(\mathfrak{T}_f + V_1 \frac{\partial \mathfrak{T}_f}{\partial \eta}.\xi\right)\begin{pmatrix} 0 \\ E_1 \end{pmatrix}\right).\delta\zeta\right]_0^1\right) dt. \end{aligned} \tag{84}$$

Now, since all the variational calculations are achieved, we can force "$\xi = \xi_d$" into the boundary term of (84) (see subsection 3.4). Hence, taking (41) into account in (84), gives the waited for "Extension of the Hamilton principle to the Cosserat beam surrounded by the stratified fluid inside $\mathcal{D}$" :

$$\int_{t_1}^{t_2}\int_0^1 \delta(\mathfrak{T}_f + \mathfrak{T}_b - \mathfrak{U}_b) \; dX_1 dt = \int_{t_1}^{t_2} \left(\delta W_{ext} - \left[\left(V_1 \frac{\partial \mathfrak{T}_f}{\partial \eta} - \mathfrak{T}_f \begin{pmatrix} 0 \\ E_1 \end{pmatrix}\right).\delta\zeta\right]_0^1\right) dt, \tag{85}$$

that replaces (4) in order to generalize the Poincaré-Cosserat equations to the L.A.E.B.T. of Lighthill.

Acknowledgment

We would like to thank the French CNRS for supporting this work through the project "Robot Anguille" of the Interdisciplinary Research Program ROBEA. We acknowledge the constructive remarks of the reviewers, which have contributed to improve the quality of this paper.

Références

[1] F. Boyer, M. Porez, and W. Khalil. Macro-continuous computed torque algorithm for the three-dimensional eel-like robot. *IEEE J. Trans. on Robotics*, 22 :763–775, 2006.

[2] K. A. McIsaac and J. P. Ostrowski. A geometric approach to anguilliform locomotion modelling of an underwater eel robot. In *IEEE Int. Conf. on Robotics and Automation, Detroit, USA*, volume 4, pages 2843–2848, 1999.

[3] H. Yamada, S. Chigisaki, M. Mori, K. Takita nd K. Ogami, and S. Hirose. Development of amphibious snake-like robot acm-r5. *the Proc. of 36th Int. Symposium on Robotics ISR2005 Japan*, 2005.

[4] A.J. Ijspeert, A. Crespi, and J-M. Cabelguen. Simulation and robotics studies of salamander locomotion. applying neurobiological principles to the control of locomotion in robots. *Neuroinformatics*, 5 :171–196, 2005.

[5] J. E. Colgate and K. M. Lynch. Mechanics and control of swimming : a review. *IEEE J. of Oceanic Engineering*, 29 :660–673, 2004.

[6] Q. Liu and K. Kawachi. A numerical study of undulatory swimming. *J. of Computational Physics*, 155 :223–247, 1999.

[7] J. Carling, T. L. Williams, and G. Bowtell. Self-propelled anguilliform swimming : simultaneous solution of the two-dimensional navier-stokes equations and newton's laws of motion. *J. Experimental Biology*, 201 :3243–3166, 1998.

[8] D. J. J. Farnell, T. David, and D. C. Barton. Numerical model of self-propulsion in a fluid. *J. of Royal Society Interface*, 2 :79–88, 2005.

[9] A. Leroyer and M. Visonneau. Numerical methods for ranse simulations of a self-propelled fish-like body. *J. of Fluids and Structures*, 20 :975–991, 2005.

[10] S. J. Hill. *Large amplitude fish swimming*. PhD thesis, University of Leeds, 1998.

[11] M. J. Wolfgang. *Hydrodynamics of flexible-body swimming motions*. PhD thesis, Massachsetts Institute of technology, 1999.

[12] J-Y. Cheng and G. L. Chahine. Computational hydrodynamics of animal swimming : boundary element method and three-dimensional vortex wake structure. *Comparative Biochemistry and Physiology*, 131 :51–60, 2001.

[13] J. Lighthill. Note on the swimming of slender fish. *J. Fluid Mechanics*, 9 :305–307, 1960.

[14] T. Y-T. Wu. Swimming of a waving plate. *J. Fluid Mech.*, 10 :321–355, 1961.

[15] M. M. Munk. The aerodynamic forces on airship hulls. *National Advisory Commitee for Aeronautics*, 184, 1924.

[16] J. Lighthill. Aquatic animal propulsion of high hydro-mechanical efficiency. *J. Fluid Mechanics*, 44 :265–301, 1970.

[17] J. Gray. Studies in animal locomotion. vi. the propulsive powers of the dolphin. *J. Experimental Biology*, 13 :192–199, 1936.

[18] F. Boyer, M. Porez, and A. Leroyer. Fast dynamics of an eel-like robot, comparisons with navier-stokes simulations. *Submitted, internal report of Ecole des Mines de Nantes no. 07/9/Auto, online available : http ://www.irccyn.ec-nantes.fr/hebergement/Publications/2007/3722.pdf*, 2007.

[19] T. McMillen and P. Holmes. An elastic rod model for anguilliform swimming. *J. Mathematical Biology*, 53 :843–886, 2006.

[20] H. Poincaré. Sur une forme nouvelle des équations de la mécanique. *Compte rendu de l'académie des sciences de Paris*, 132 :369–371, 1901.

[21] V. I. Arnold. Sur la géométrie différentielle des groupes de lie de dimension infinie et ses applications à l'hydrodynamique des fluides parfaits. *Annales de l'institut J. Fourier*, XVI :319–361, 1966.

[22] D. G. Ebin and J. E. Marsden. Groups of diffeomorphisms and the motion of an incompressible fluid. *Ann. Mathematical*, 92 :102–163, 1970.

[23] J. P. Ostrowski. Computing reduced equations for robotic systems with constraints and symmetries. *IEEE Trans. on Robotics and Automation*, 15 :111–123, 1999.

[24] D. K. Kelly and R. M. Murray. Modeling efficient pisciform swmming for control. *J. Nonlinear and Robust Control*, 10 :217–241, 2000.

[25] E. Kanso, J. E. Marsden, C. W. Rowley, and J. Melli-Huber. Locomotion of articulated bodies in a perfect planar fluid. *J. of Nonlinear Science*, 15(4) :255–289, 2005.

[26] J. B. Melli, C. W. Rowley, and D. S. Rufat. Motion planning for an articulated body in a perfect fluid. *SIAM J. on Applied Dynamical Systems*, 5 :650–669, 2006.

[27] F. Boyer and D. Primault. The poincaré-chetayev equations and flexible multibody systems. *J. of Applied Mathematics and Mechanics*, 69 :925–942, 2005.

[28] G. I. Taylor. Analysis swimming long narrow animals. *Proc. of the Royal Society of London, series A : Mathematical and physical sciences*, 214 :158–183, 1952.

[29] J. Lighthill. Large-amplitude elongated body theory of fish locomotion. *Proc. of Royal Society*, 179 :125–138, 1971.

[30] J. C. Simo. A finite strain beam formulation. the three-dimensional dynamic problem. part i : Formulation and optimal parametrization. *Computer Methods in Applied Mechanics and Engineering*, 72 :267–304, 1985.

[31] L. Meirovitch. *Methods of analytical dynamics.* Mc.Graw-Hill, New-York, 1970.

[32] V. I. Arnold. *Mathematical methods in classical mechanics.* Springer-Verlag, 1988.

[33] F. Boyer and D. Primault. Finite element of slender beams in finite transformations - a geometrically exact approach. *Int.l J. of Numerical Methods in Engineering*, 59 :669–702, 2004.

[34] J. E. Marsden and T. S. Ratiu. *Introduction to mechanics and symmetry, scnd. Ed.* Springer, 1999.

[35] E. Reissner. On a one-dimensional large displacement finite-strain theory. *Studies Applied Mathematics*, 52 :87–95, 1973.

[36] J. C. Simo and L. Vu-Quoc. On the dynamics in space of rods undergoing large motions. a geometrically exact approach. *Computer Methods in Applied Mechanics and Engineering*, 66 :125–161, 1988.

[37] W. Khalil and E. Dombre. *Modeling, Identification and Control of Robots.* Penton-Sciences, 2002.

[38] J. Y. S. Luh, M. W. Walker, and R. C. P. Paul. On-line computational scheme for mechanical manipulator. *Trans. of ASME, J. of Dynamic Systems, Measurement, and Control*, 102 :69–76, 1980.

[39] R. Featherstone. The calculation of robot dynamics using articulated-body inertias. *Int. J. of Robotics Research*, 2 :13–30, 1983.

[40] R. Featherstone and D. Orin. Robot dynamics : equation and algorithms. In *IEEE Int. Conf. on Robotics and automation, San Francisco, USA*, volume 1, pages 826–834, 2000.

[41] G. K. Batchelor. *An Introduction To Fluid Dynamics.* Cambridge University Press, 1967.

[42] Horace Lamb. *Hydrodynamics.* Dover Publication, 1932.

[43] G. del Valle, I. Campos, and J. L. Jiménez. A hamilton-jacobi approach to the rocket problem. *Europeen J. of Physics*, 17 :253–257, 1996.

[44] S. F. Hoerner. *Fluid Dynamics Drag.* Hoerner Fluid Dynamics, 1965.

[45] M. J. Ringuette. *Vortex formation and drag on low aspect ratio, normal flat plates.* PhD thesis, California Institute of technology, Pasadena, California, 2004.

[46] G. Susbielles and Ch. Bratu. *Vagues et Ouvrages Pétroliers en Mer.* Editions Technip Paris, 1981.

[47] C. M. Breder. The locomotion fishes. *Zoologica, New York*, 4 :159–256, 1926.

[48] J. Gray. Studies in animal locomotion. i. the movement of fish with special reference to the eel. *J. Experimental Biology*, 10 :88–104, 1933.

[49] J. Lighthill. *Mathematical biofluiddynamics.* S.I.A.M., 1975.

[50] M. Alamir, M. El-Rafei, G. Hafidi, N. Marchand, M. Porez, and F. Boyer. Feedback design for 3d movement of an eel-like robot. In *IEEE Inter. Conf. on Robotics and Automation, Rome, Italia*, pages 256–261, 2007.

[51] J. C. Simo and L. Vu-Quoc. A three-dimensional finite-strain rod model. part ii : Computational aspects. *Computer Methods in Applied Mechanics and Engineering*, 58 :79–116, 1986.